3 Optical Aspects on EOCB

3.1 Introduction

In the optical communication field, polymethylmethacrylate (PMMA), polystyrene (PS), polycarbonate (PC), epoxy, polyimide, perfluorocyclobutyl (PFCB)-based polymers, and polysiloxane etc. have been widely used as multimode waveguides materials for short-distance datacom applications, e.g., with polymer optical fibres (POF) in filtering and routing devices and others. However, their implementation in applications for the datacom market is still critical and restricted due to various factors such as high cost, shrinking, thermal instability etc., despite the fact that these materials all show the required optical transparency in the common datacom region (600 - 1600 nm).[45-53] Recently, two component addition curing polysiloxane e.g. Polydimethylsiloxane (PDMS), frequently referred to by the generic name silicones, are polymers with a unique combination of properties resulting from the presence of an inorganic siloxane backbone and organic methyl groups attached to silicon. Thermally robust SiO units are the backbone of those materials and thermal stability can be up to 300 °C, their refractive indices can range from 1.39 to 1.50 (at a wavelength of 589 nm at 20 °C) by varying the concentration of vinyl groups in the base component.[53-55] The chemical configuration produces silicone polymers which have low glass transition temperatures, and hence are fluids over a wide range of temperatures, have good thermal stability, good oxidative resistance, good optical properties down to 300 nm and good chemical stability. In addition, due to easy and low cost (≤ 50 euro/ l) thermal casting and injection techniques under no shrinking, and also such PDMS show minimal insertion loss compared to multimode PMMA and glass waveguides, thus they were received much interest for application in waveguide based devices.

The bands in the spectral VIS-NIR region are primarily overtones and combinations of the fundamental bands found in the classical mid-infrared region. Most chemical bonds have negligible harmonic absorption compared with so-called X-H subgroup

bonds, i.e., C-H, N-H and O-H. Among the latter, the absorption losses from N-H and O-H subgroups are usually 10 - 20 times larger than those arising from C-H vibrations, so for the pre-selection of optical siloxane-based polymers, no N-H and O-H bonds should exist. With the growing interest in addition-thermal curing two-component siloxane-based materials for optical datacom applications e.g. EOCB production project: Prospeos, however, until now only very few reports have been devoted to the characterization of their optical characteristics in the visible and near-infrared (VIS - NIR) region, which is the most important wavelength range for datacom and telecom applications.

In this chapter, commonly used PDMS –also practically applied materials in EOCB prospeos project- was selected for this study with regard to the bandwidth applicability. An empirical equation for estimating the wavelengths with the most significant intrinsic absorption loss due to the corresponding vibration band was formulated, which was found to agree well with the experimental data. It provides a relationship between the integral band strength and the intrinsic absorption loss, thus furnishing us with estimates of the loss limit in such materials when implementation in data- and telecom devices is strived for. For such purpose, singlemode and multimode waveguides were fabricated and their respective optical insertion loss was also measured at 1300 nm and 850 nm, as well their thermal stability verified.

3.2 Experimental

Polymer formulation

The key functional group of the PDMS polymers is $–SiO(CH_3)_2$ which can be considered as an organically modified quartz, i.e., two oxygen atoms attached to every silicon atom have been replaced by methyl groups. This changes the structure from the three-dimensional backbone of quartz to linear polymer molecules. Here, the methyl groups are free to rotate about the -Si-O-Si- chain. As a derivative, other groups instead of methyl groups can be attached to the silicon-oxygen backbone. The linear silicone polymers can be crosslinked to each other by different extents, i.e., covalently via groups containing different atoms. This explains the wide range of optical, mechanical and chemical properties of the corresponding silicones.

A two-component commercial PDMS polymer called RT 601 (Wacker Chemie, Burghausen, Germany) was used as cladding material. In close cooperation with

our group, the PDMS core material was especially developed by Wacker Chemie (provisional product name SLM 77522), with a few methyl groups substituted by phenyl groups for obtaining a higher refractive index as required for waveguiding. Both materials were prepared from two components by means of a cross-linking procedure through a hydrosilylation reaction by thermal curing using a platinum catalyst. The addition reaction occurs mainly on the terminal carbon and is catalysed by organometallic Pt colloid complexes. The following mechanism, as illustrated in Fig. 3.1, has been proposed after the oxidative addition of the SiH groups in the coupling agent by means of the Pt catalyst with a following hydrogen transfer onto the double bond and a reductive elimination in the product (for simplification, other Pt ligands and Si-substituents are omitted).

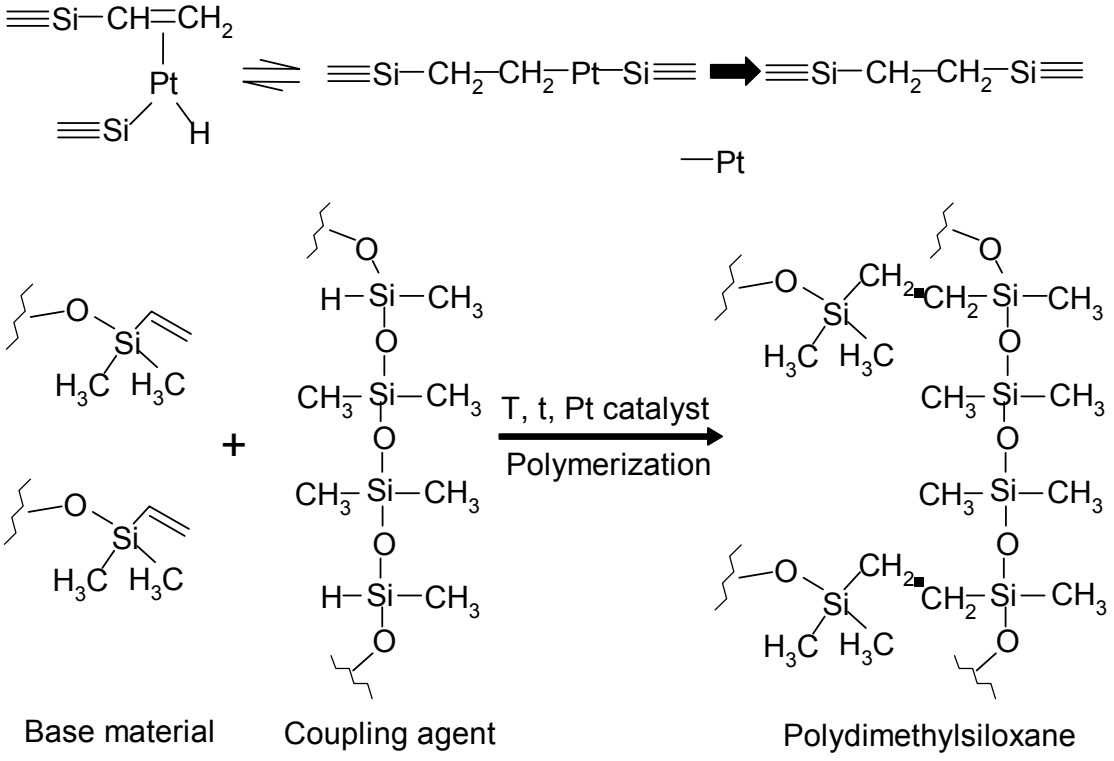

Fig. 3.1 *PDMS polymerisation scheme based on a two-component set. The first scheme illustrates the reaction principle (the symbol in the above formula '≡' represents two methyl groups and the rest of the polymer chain).*

To study the optical properties of amorphous PDMS cladding and core polymers, it was necessary to purify the raw material before the curing process to avoid extrinsic losses, e.g., by particle scattering. The base material and coupling agent were both filtered using a cellulose-mixester membrane filter of pore size of 0.2 µm. After purification, they were mixed in the ratio of 19:1 for cladding and 9:1 for

core materials, respectively, and deaerated through vacuumizing. Subsequently, the mixed polymers were cured in a clean oven for 2 hrs at 70 °C to obtain samples for the optical characterisation. All experiments were performed under clean room (class 100 and 10) conditions.

Spectrometers used for optical characterisation

For mid-infrared measurements, a PE-2000 FTIR-Spectrometer (Perkin-Elmer, Überlingen, Germany) was available. As measurement conditions, 500 scans were coadded for spectral recording at a spectral resolution of 2 cm^{-1}. Transmission measurements were carried out with solid films on a ZnSe window. Near-infrared and visible optical absorption measurements were made using a FT-NIR-spectrometer Vector 22N from Bruker Optics (Ettlingen, Germany) equipped with a Ge-diode as detector (1500 scans coadded, spectral resolution of 64 cm^{-1} and Norton-Beer (strong) apodization) and, secondly, a spectrometer Cary 5 from Varian (Darmstadt, Germany), based on a scanning double monochromator (scan rate 60 nm/ min; slit width 2 nm). Samples were prepared with optically flat surfaces, and their thickness varied between 3 mm and 30 mm. The measurements were carried out in a temperature controlled environment of 23 ^{o}C ± 2 °C.

For Raman measurements, a portable HoloSpec Raman spectrometer from Kaiser Optical Systems, Inc., provided with a diode laser (λ = 785 nm, 50 mW) from SDL, Inc. and a liquid-N_2 cooled CCD detector from RS Roper Scientific were used. Part of the spectrometer is a non-scanning polychromator that is equipped with a fiber-optic probe, usable also for remote-measurements. It combines robustness and high detectivity with reasonable resolution. The following measurement conditions were used: integration time of 25 s with 10 spectral frame accumulations at a laser power of 10 mW.

Refractive index measurements

Wavelength dependent measurements in the visible and near-infrared spectral range were carried out on RT 601 PDMS intended as cladding and SLM 77522 as core material. An "ABBE-Refractometer" from Zeiss (Jena, German.) was applied to measure the different refractive indices by using the limit angle of total reflection at different wavelengths. For this, a sodium emission lamp with filter at 589 nm was used, and a halogen tungsten lamp with different filters at 515 nm, 632 nm, 852 nm, 1300 nm and 1550 nm, respectively, under a constant temperature of 20 °C.

3.3 Refractive Index and Bandwidth

Optical waveguiding was first referred to as ‘light piping’ in 1880 by Wheeler. This effect of light transmitted through a glass pipe medium is what is now described with fibre-optics technology. Guided wave optics confines radiation in the optical waveguides through the phenomenon of total internal reflection (TIR), where the core material is surrounded by a cladding material with a lower refractive index. The coupling and propagation characteristic of the waveguide is thus defined by the core-cladding index difference.

The refractive index of polymers mainly depends on the molecular polarizability, the molecular volume and the difference between the used optical wavelength and the maximum absorption wavelength of polymers. In terms of the PDMS polymer used in the paper, the core material has an intrinsic higher refractive index than the cladding material through the introduction of phenyl groups that are substituting methyl groups in the side chain of the PDMS backbone which will be described in detailed elsewhere. The ratio of methyl to phenyl units can be varied to obtain a broader refractive indices interval. [56]

With the refractive indices measured at several wavelengths, there are various dispersion formulas available that could be used for the fitting refractive index data, e.g., equations provided by Hartman, Conrady, Herzberger, Schott Optical Glass, Inc., and Sellmeier.[57-59] But some of the formulas, e.g., by Conrady, Schott or Herzberger, are linear in their fitting constants, which means they can be fitted easily using a classical least-squares procedure; from this, it should be clear that the fitting accuracy should be the dominant aspect in choosing the most appropriate dispersion formula. From this point of view, the Sellmeier equation is especially suited for the coverage of the refractive index in the wavelength range from the UV through the visible to the mid-IR range (up to 2.3 μm) due to its high accuracy and applicability. The Sellmeier formula is derived from the classical dispersion theory and allows the description of the progression of refractive index throughout the total transmission region with one set of parameters and the calculation of accurate interpolated values. Presently, it has been found that a 3-term Sellmeier formula is generally a necessary and sufficient descriptor for satisfactorily fitting almost all refractive index data of materials in practical use within their main transparent region. Equation (3.1a) describes the three-term Sellmeier formula:

$$n^2 = 1 + \frac{B_1 \lambda^2}{\lambda^2 - C_1} + \frac{B_2 \lambda^2}{\lambda^2 - C_2} + \frac{B_3 \lambda^2}{\lambda^2 - C_3} \qquad (3.1a)$$

where n is the optical index at wavelength λ, B_1 - B_3 and C_1 - C_3 are the constants to be determined by the fitting process.

In Fig. 3.2A and B, the refractive index measurement results of the cladding and core PDMS materials with the Sellmeier fitting curves and the calculated A_N values (numeric aperture, $A_N = \sqrt{n_{core}^2 - n_{cladding}^2}$) at different wavelengths are shown, respectively. The Sellmeier formular for the two fitting curves of cladding and core are shown in equations 3.1b and 3.1c.

$$n^2 = 1 + \frac{-2.30744 \cdot \lambda^2}{\lambda^2 + 0.02605} + \frac{1.85952 \cdot \lambda^2}{\lambda^2 + 0.01362} + \frac{1.39944 \cdot \lambda^2}{\lambda^2 + 0.01349} \qquad (3.1b)$$

$$n^2 = 1 + \frac{-0.1432 \cdot \lambda^2}{\lambda^2 + 0.69379} + \frac{1.01366 \cdot \lambda^2}{\lambda^2 - 0.01304} + \frac{0.14158 \cdot \lambda^2}{\lambda^2 + 0.58129} \qquad (3.1c)$$

In addition, by varying the temperature from 20 °C to 55 °C the respective thermo-optic coefficients (TOC) of core and cladding were obtained and displayed in Fig. 4, where the core TOC is $-3.59 \cdot 10^{-4}$/ K and that of the cladding material is $-3.65 \cdot 10^{-4}$/ K. Whilst as seen, the A_N values are quite stable with a rise in temperature, for the PDMS waveguides the temperature is possibly not stable enough due to environmental changes and variation from active elements, e.g. the optical laser and photodiode etc.

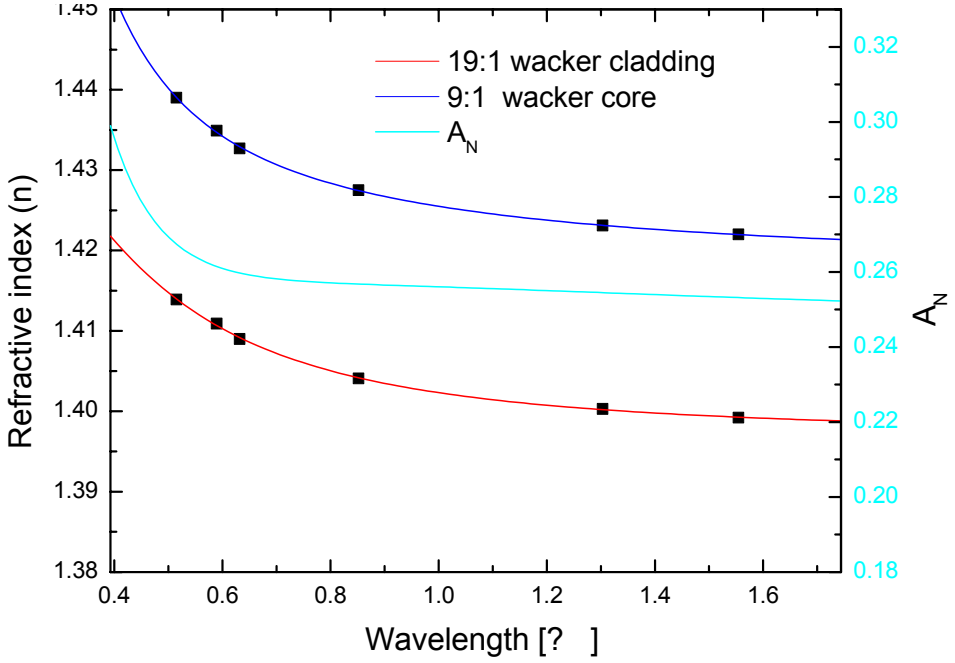

Fig. 3.2*A* *Wavelength dependency of the refractive indices of the PDMS core and cladding materials (left ordinate scale) and the numerical aperture calculated for this combination of materials (right ordinate scale);*

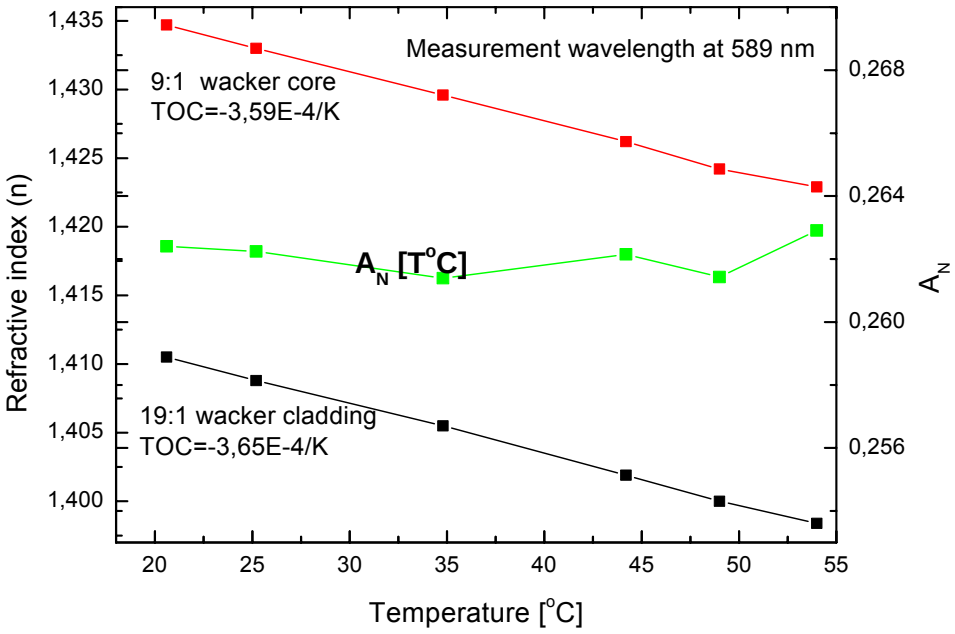

Fig. 3.2B *Temperature dependence for the refractive indices of both materials and of the corresponding numerical aperture at 589 nm.*

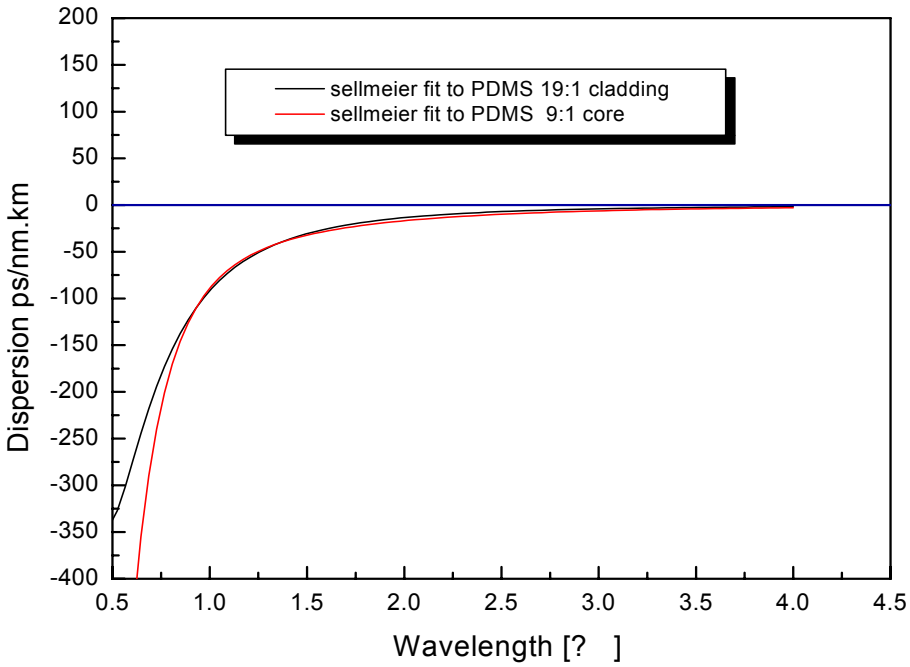

Fig. 3.3 *Calculated wavelength dependent dispersion for PDMS clad and core materials*

In optical waveguides, mode dispersion (different propagation constants for each mode) and material dispersion are the main effects which limit the bandwidth of the optical waveguide transmission. Based on the obtained Sellmeier fitting curves, as shown in Fig. 3.2A, the material dispersion curves of the PDMS cladding and core were both obtained using the material dispersion equations below (c/n is the light velocity).

$$M(\lambda) = -(\frac{n \cdot \lambda}{c}) \cdot (\frac{d^2 n}{d\lambda^2}) \qquad (3.2)$$

As seen, the material dispersion of the core PDMS is -144.9 ps/ (nm.km) and -45.01 ps/ (nm.km) and of the clad material is -136.87 ps/ (nm.km) and -45.96 ps/ (nm.km) at 850 and 1300 nm wavelengths, respectively.

For multimode waveguides, apart from the material dispersion, there also exists mode dispersion, which is the maximal time delay $\Delta t_{g\max}$ between the longest and shortest rays through the core of the PDMS waveguide. This can be expressed by Eq.3.3:[4]

$$\Delta t_{g\max} = LA_N^2/(2cn_{core}), \qquad (3.3)$$

where L is the length of the polymer waveguide layer, A_N is numeric aperture of the

step-index waveguide, c is the light speed in vacuum and n_{core} is the refractive index of the core material at the work wavelength.

Also, the relation between dispersion and bandwidth may be simplified with Eq. 3.4:

$$B \gg 0,443/\Delta t_{g\max} \qquad (3.4)$$

According to the Nyquist rule[60] the maximum data rate is $R_{\max} = 2B\log_2 V$ bps where B is the bandwidth and V is the number of states encoded. In our case is V=2, so $R_{\max} = 2B$, with B and Δt substituted equation (3.4) and (3.3), respectively, leading to,

$$R_{\max} = \frac{1.772 \cdot c \cdot n_{core}}{L \quad A_N^2} \qquad (3.5)$$

For such a PDMS waveguide system, assuming a transmission speed of 10 Gbps at 850 nm wavelength and a 20 °C work temperature, it can be concluded that its optical pathway should be below 1.14 m, which is the precondition for using such PDMS polymers for optical waveguiding. If longer optical interconnect is required, the material design can be achieved through varying the ratio of phenyl and methyl groups in PDMS to decrease the index difference between core and cladding material.[53, 61]

3.4 Optical Loss

In general, all optical waveguide devices need to have low optical loss, in particular at the major communication wavelengths, e.g. 850 and 980 nm for datacom, or 1310 and 1550 nm for telecom applications. Normally, four kinds of attenuation loss phenomena contribute to the propagation loss in optical polymer materials within the VIS - NIR region: first, in the far ultraviolet region with a wavelength less than 200 nm the molecules with single bonds (predominantly molecular groups with aliphatic hydrogen atoms) can undergo σ fi σ* transitions, but this is not of interest to us. In addition there are absorptions arising from p fi p* or n fi p* electronic transitions caused by double bond structural units, e.g., >C=C< or >C=O etc. Theses usually appear in the ultraviolet wavelength region and influence the propagation loss of optical polymer materials still in the visible wavelength region through their absorption tails (200 - 400 nm). Secondly, molecular vibration absorption exists due to the higher harmonics (overtones) of fundamental

stretching vibrations and combination bands with corresponding bending vibrations, which are main contributors to the absorption losses as found in amorphous polymers at wavelengths beyond 600 nm. Furthermore, the third significant loss factor is due to Rayleigh scattering, caused by fluctuations of the density and the refractive index in such polymer materials. The three loss phenomena mentioned above explain intrinsic propagation losses. Other sources that are responsible for extrinsic loss can be traced back to contaminating dust, pores and crystallites from the fabrication process. Of particular importance, especially for polymer waveguide systems, is the scattering due to the core–clad interface roughness as another source of extrinsic loss.[62]

3.4.1 Scattering Loss

Extrinsic loss arising from scattering in polymers can result from unfiltered particles, dust, dissolved bubbles and uncreated monomer. For eliminating this source of extrinsic scattering it is necessary to follow rigorously ultimate procedures in the preparation of polymer formulations, e.g. by filtering and deaeration etc., and to perform all preparations in a clean room environment.

As scattering often arises from a number of sources, the experimental scattering data often fits with an empirical law of the form: [56]

$$a_{scatter} = A + B/\lambda^2 + C/\lambda^4 \qquad (3.6)$$

where A is the contribution from large particle scattering (i.e., with their diameters >> λ), B the contribution from inhomogeneities in the order of λ in size (Mie scattering), and C the contribution from smaller inhomogeneities (size << λ, Rayleigh-like).

The material of RTV 2 PDMS is a kind of elastomer polymer with a very low glass-transition temperature (around – 50 ^{o}C) which means that it is in the liquid state at the normal operation temperature. In addition, its base components have been filtered and deaerated before thermal curing, so Rayleigh scattering loss will be negligible compared with other intrinsic losses, e.g. from vibrational overtone absorptions beyond 600 nm.

Then RTV 2 PDMS is polymerized through a hydrosilation reaction by thermal curing using a platinum catalyst (see also Fig. 3.1) and after hydrosilylation, the Pt catalyst complex will be a by-product. The Pt catalyst complex is possibly bonded with some left over polar components in cured PDMS, e.g. vinyl groups as found in

the base component to form a more stable and larger size colloid with increasing temperature and continuous curing. This will result in PDMS compositional inhomogeneities in even larger length scales giving rise to optical scattering. To investigate and confirm the influence of Pt on the optical loss, a commercial Pt catalyst complex (Catalyst EP from Wacker, Chemie) and a pure filtered PDMS polymer (RT 601, Wacker, including 30 - 40 ppm of Pt in the base component), not containing other impurities like silicon oil and inhibitors etc., were selected for studying its contribution to the loss budget.

It was identified in Fig. 3.4A that the optical scattering loss of PDMS increased gradually as a larger platinum concentration was chosen. From Fig.3.4B, it was also found that Pt colloids changed peak shifts from 260 nm to 325 nm due to size change or so due to more platinum catalyst added and higher temperature treatment. Whilst it also proves that PDMS with the increased addition of Pt catalyst shows brownness and yellowness due to the blue light scattered out. In order to improve the PDMS optical stability and decrease the scattering loss, the Pt concentration should get controlled in a preliminary step before reaching its final applications.

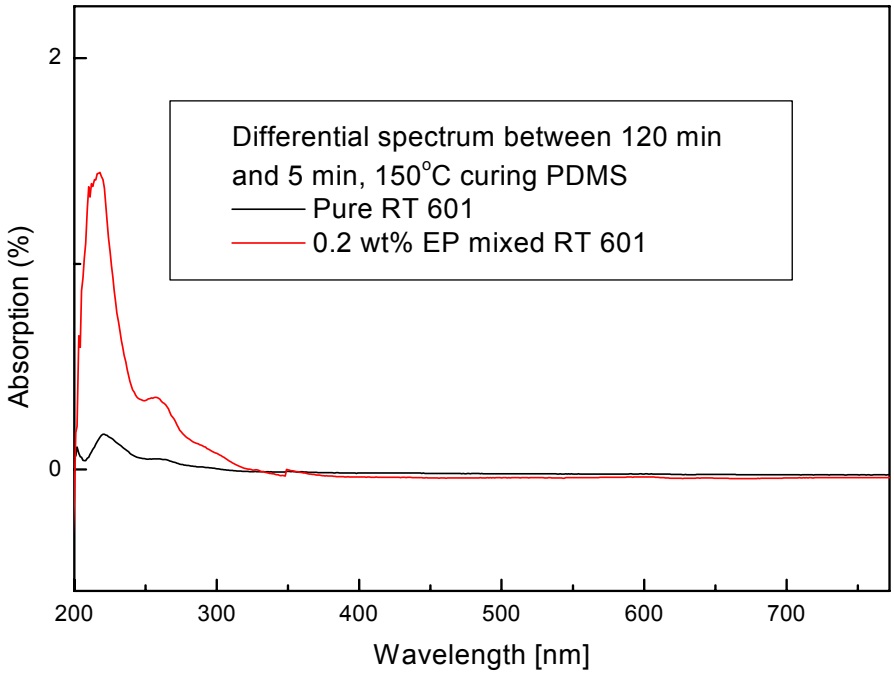

Fig. 3.4 A *optical scattering loss of PDMS with different Pt concentrations;*

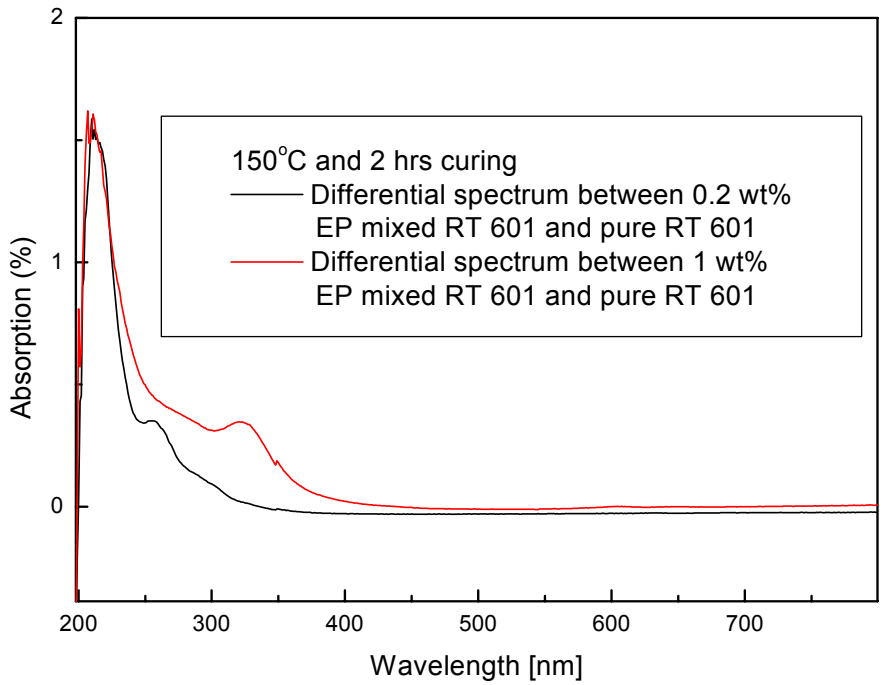

Fig. 3.4 B *size change due to different Pt concentrations*

3.4.2 Intrinsic Absorption Loss by Molecule Vibrations

For polymer materials, both electronic and vibrational absorptions are likely to contribute to optical loss. Polymeric media generally have large absorptions in the ultraviolet owing to fundamental excitations of their electrons. These absorptions tend to be in the deep ultraviolet (less than 200 nm) for polymers with predominantly aliphatic hydrogen atoms, and in the near UV ranging from 200 to 400 nm for polymers with significant numbers of aromatic hydrogens.

Then in the VIS-NIR region, absorptions coming from overtones and combinations of the fundamental bands found in the classical mid-infrared region are dominant. Since the strength of the absorption tends to decrease by approximately an order of magnitude between each harmonic order, higher harmonics are generally weak enough to not be of concern (at least for waveguide applications). Clearly, the highest energy vibrations will be those that have high spring constants (stiff bonds, such as double bonds) or small reduced masses. The smallest reduced mass occurs when one of the atoms is hydrogen. Thus for most chemical bonds, they have negligible harmonic absorption compared with some X-H bonds (C-H, N-H and O-H), in addition among them the absorption losses from N-H and O-H are 10-20 times larger than C-H, so in the pre-selection of optical polymers, they

should contain less N-H and O-H bonds.[53]

Determination of the anharmonicity constants of PDMS

PDMS system as studied belongs to the category of addition thermal curing RTV 2 silicone resins, and after polymerization electronic transition absorption can be neglected in the optical loss analysis of PDMS after 600 nm wavelengths. In addition, once Pt concentration is controlled in from 10 to 50 ppm which can ensure the basic curing of PDMS, consequently, most of the intrinsic attenuation losses of PDMS arise from overtone and combination bands of molecular vibrations.

From mid-IR spectra of cladding and core were, the band assignment of measured with FTIR and FTRaman spectroscopies and illustrated in Fig. 3.5, furthermore we assigned the fundamental bands of various chemical bonds in PDMS e.g. Si-O and Si-C etc., respectively, which are observed at longer wavelength in the mid-IR region and shown in Table 3.1. Absorption bands due to these chemical bonds can be neglected in the VIS-NIR wavelength region, compared with vibrations of the C-H bonds within them, e.g. polyatomic $–CH_3$ methyl, $-CH_2$ methylene and C=C vinyl and CH phenyl (in core material- SLM 77522) groups etc.

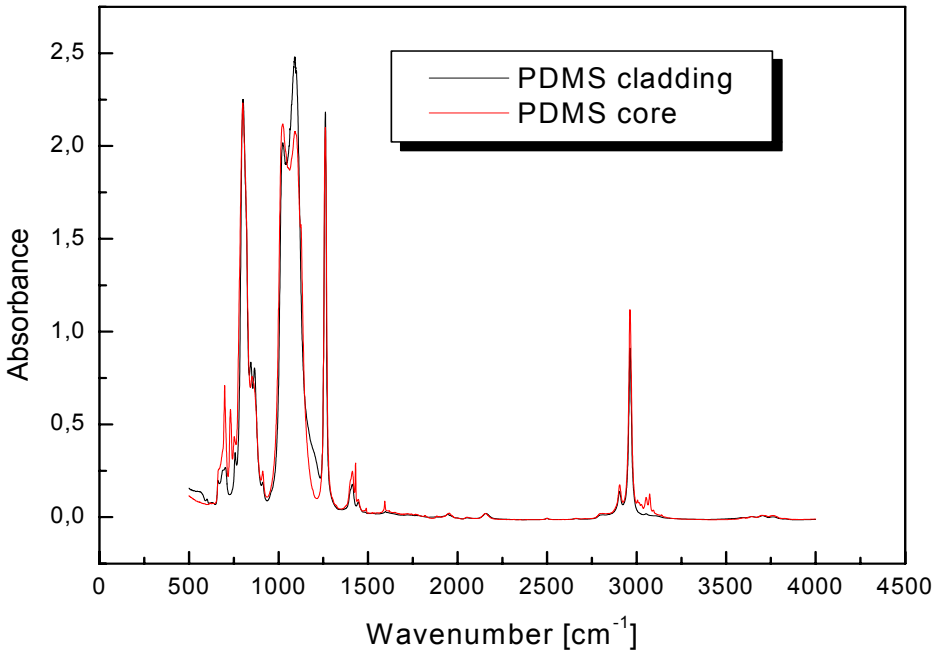

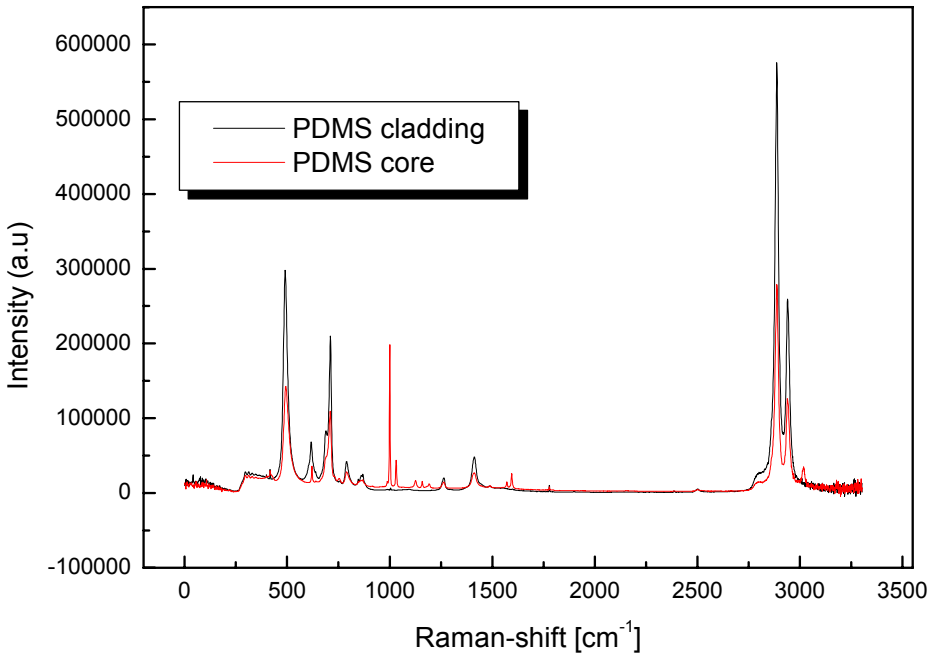

Fig. 3.5 *FTIR and FTRaman spectra of clad and core PDMS*

To polyatomic molecules, the anharmonicity causes not only the appearance of overtones but combination bands as well. When the fundamental are related to C-H, N-H and O-H functional groups that occur between 4000 and 2500 cm^{-1}, the overtones and combinations make up the backbone of what is called the "near-infrared". Thus this region of the spectrum is not really difficult and can be predicted by the rules of spectroscopy as well as any other "normal" region.

Table 3.1 *Infrared and Raman spectral bands assignment of PDMS* [63-64]

Assignment	Cladding ($\tilde{n}_{exp}$ /cm^{-1})	Core ($\tilde{n}_{exp}$ /cm^{-1})
Si-C - Valence, sy, $Si(CH_3)_2$	664	664
Si-C - Valence, as, $Si(CH_3)_3$	687	687
CH_3 - rocking, sy, $Si(CH_3)_3$	758	758
Si-C - Valence, as, $Si(CH_3)_2$	799	799
CH_3 - rocking, sy, $Si(CH_3)_2$	815	815
CH_3 - rocking, as, $Si(CH_3)_3$	844	844

CH_3 - rocking, as, $Si(CH_3)_2$	866	866
Si-C stretching and CH_3 rocking	802	800
CH_2 wag	912	911
Si-O-Si stretching vibration.	1023-1100	1024-1100
$\delta_s(CH_3)$	1263	1261
CH_2 asymm waging	1342	1337
CH_2 symm waging, C-C stretching	1367	1372
$\delta_{as}(CH_3)$	1412	1412
Si-Phenyl	ND	1430
CH_2 symm. Bending	1446	1446
CH_2 asymm. Bending	1475	1479
Si-CH=CH_2	1597	1593
Si-H	2159	2156
$n_s(CH_3)$	2905	2905
$n_{as}(CH_3)$	2963	2963
$n_s(CH_2)$	2840	2840
$n_{as}(CH_2)$	2928	2928
$n_s(=CH_2)$	2970	2970
$n_{as}(=CH_2)$	3041	3043
aromatic $n_s(CH)$ stretching	ND	3052
aromatic $n_{as}(CH)$ stretching	ND	3072

Taking into account the anharmonicity terms (higher than quadratic terms, cubic, quartic…), the general formula (without degenerate vibrations) for combination and overtone vibrational energy levels of a polyatomic group (term scheme is given in wavenumber units) is: [63]

$$G(v_1, v_2 \ldots) = \sum_i \bar{n}_i \left(v_i + \frac{1}{2}\right) + \sum_i \sum_{k \neq i} X_{ik} \left(v_i + \frac{1}{2}\right)\left(v_k + \frac{1}{2}\right) + \ldots\ldots\ldots (3.7)$$

Where $\tilde{n}$ i is the corresponding frequency of the symmetrical stretching and bending, asymmetrical stretching and deformation fundamental vibrations etc. (also

called normal vibrations) measured in units of cm^{-1}, and the X_{ik} are their anharmonicity constants.

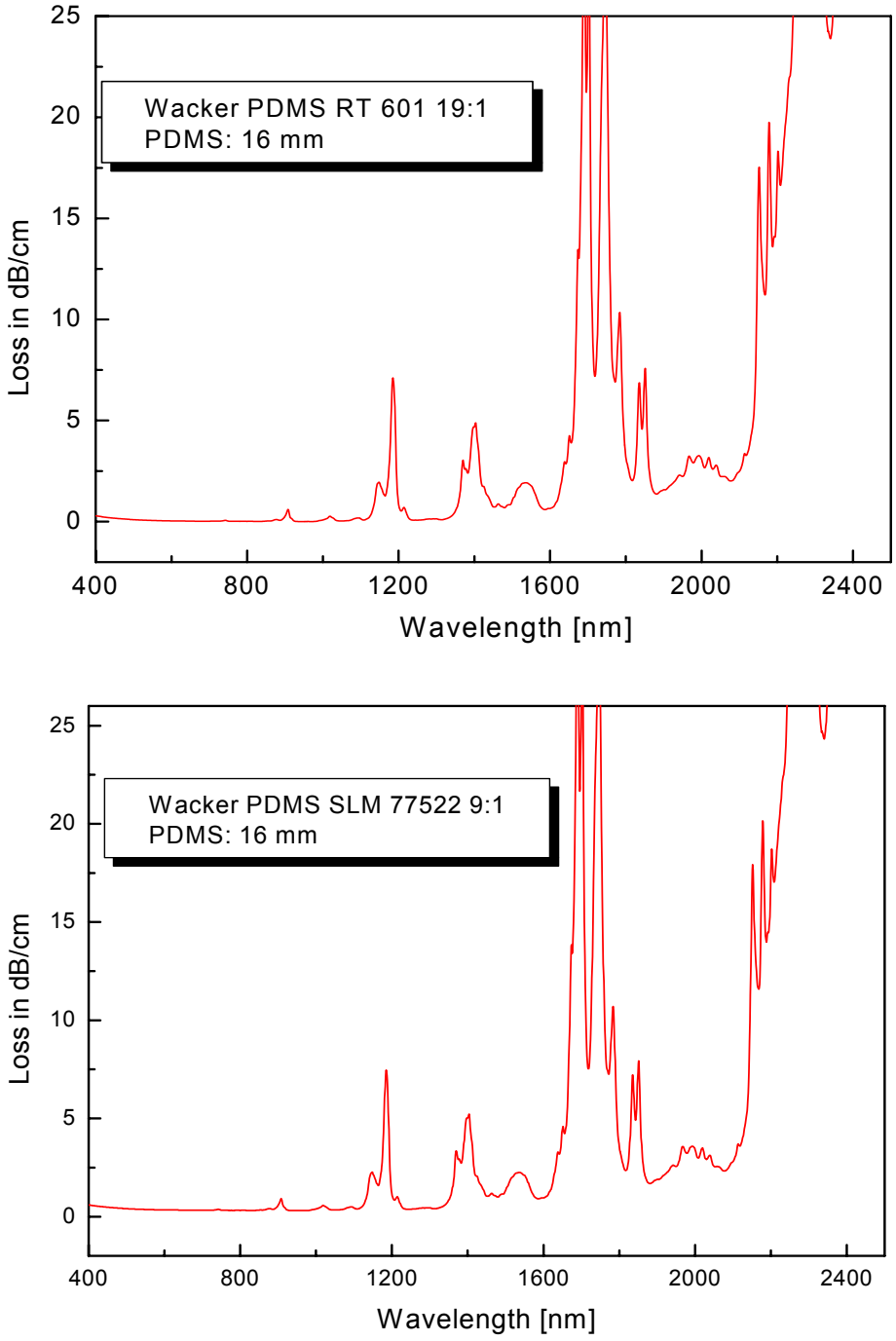

Fig. 3.6 *FTNIR loss spectra of clad and core PDMS*

CH_3 methyl group was selected for study and then the approach for determination of the anharmonicity constants is also valid to other molecular groups. For the assignment of higher overtone and combination bands, as well as the fundamental bands of the CH_3-group vibrations in cladding and core PDMS polymers, their NIR spectra were measured as well, which are presented in Fig. 3.6.

A molecule containing a number, N, atoms will have (3N-6) vibrational degrees of freedom (3N-5 for linear molecules). The PDMS molecular structure contains four atoms in the polyatomic CH_3- group, and thus the latter holds six vibrational degrees of freedom; among them, and in order to simplify the calculations, we are considering only four normal vibrations, i.e. the symmetric and asymmetric stretching and deformation vibrations, called n_1, n_2, n_3, n_4, since further two are both found at longer wavelength and show relatively low intensity. Thus, their influence on the VIS-NIR region will be negligible. With our previous assignments, we can also calculate the anharmonicity constants. For example, the wavenumber associated with the frequency of the n_1 vibration is given by the following term differences:

$$\overline{v_1^{01}} = G(1,0,0,0) - G(0,0,0,0) = \overline{v_1} + 2X_{11} + \frac{1}{2}X_{12} + \frac{1}{2}X_{13} + \frac{1}{2}X_{14} \qquad (3.8a)$$

And, for the first overtone of vibration n_1, also called $2n_1$, with $v_1 = 2$, $v_2 = 0$, $v_3 = 0$ and $v_4 = 0$:

$$\overline{v_1^{02}} = G(2,0,0,0) - G(0,0,0,0) = 2\overline{v_1} + 6X_{11} + X_{12} + X_{13} + X_{14} = 2\overline{v_1^{01}} + 2X_{11} \qquad (3.8b)$$

In the case of the CH_3-group, the fundamental $n1$ is located at 2905 cm^{-1} and its first overtone is observed at 5725 cm^{-1}, and X11 can be easily calculated:

$$X_{11} = [5725 - 2 \cdot (2905)]/2 = -42.5 .$$

With respect to combination bands, e.g. n_1+n_2, the following formula applies:

$$(\overline{v_1} + \overline{v_2}) = G(1,1,0,0) - G(0,0,0,0) = \overline{v_1^{01}} + \overline{v_2^{01}} + X_{12} \qquad (3.8c)$$

Here, the combination band n_1+n_2 is located at 5725 cm^{-1} and the two fundamentals are found at 2905 cm^{-1} and 2963 cm^{-1} respectively, and thus the coupling constant X_{12} may be easily obtained.

Altogether, the parameters from the further overtone and combination bands can be deduced by analogy and the vibrational energy levels of CH_3-group vibrations in RT 601 PDMS can be described by:

$$G(v_1,v_2,v_3,v_4) = \bar{\nu}_1(v_1+\frac{1}{2}) + \bar{\nu}_2(v_2+\frac{1}{2}) + \bar{\nu}_3(v_3+\frac{1}{2}) + \bar{\nu}_4(v_4+\frac{1}{2}) - 42.5\,(v_1+\frac{1}{2})^2 - 26.5\,(v_2+\frac{1}{2})^2$$
$$-13\,(v_3+\frac{1}{2})^2 + 4.5\,(v_4+\frac{1}{2})^2 - 143\,(v_1+\frac{1}{2})(v_2+\frac{1}{2}) - 4\,(v_1+\frac{1}{2})(v_3+\frac{1}{2}) \qquad (3.9)$$
$$+7.5\,(v_1+\frac{1}{2})(v_4+\frac{1}{2}) - 10\,(v_2+\frac{1}{2})(v_3+\frac{1}{2}) - 4\,(v_2+\frac{1}{2})(v_4+\frac{1}{2}) - 5\,(v_3+\frac{1}{2})(v_4+\frac{1}{2})$$

The vibrational energy level of CH_3-group vibrations in SLM 77522 PDMS is obtained with the same approach and can be described by:

$$G(v_1,v_2,v_3,v_4) = \bar{\nu}_1(v_1+\frac{1}{2}) + \bar{\nu}_2(v_2+\frac{1}{2}) + \bar{\nu}_3(v_3+\frac{1}{2}) + \bar{\nu}_4(v_4+\frac{1}{2}) - 42.5\,(v_1+\frac{1}{2})^2 - 26.5\,(v_2+\frac{1}{2})^2$$
$$-11\,(v_3+\frac{1}{2})^2 + 8.5\,(v_4+\frac{1}{2})^2 - 143\,(v_1+\frac{1}{2})(v_2+\frac{1}{2}) - 2\,(v_1+\frac{1}{2})(v_3+\frac{1}{2}) \qquad (3.10)$$
$$+1.5\,(v_1+\frac{1}{2})(v_4+\frac{1}{2}) - 8\,(v_2+\frac{1}{2})(v_3+\frac{1}{2}) - 6\,(v_2+\frac{1}{2})(v_4+\frac{1}{2}) - 5\,(v_3+\frac{1}{2})(v_4+\frac{1}{2})$$

From the equations above, we can calculate the wavenumbers of overtone and combination bands of CH_3-group vibrations from 600 nm to 1800 nm in such two PDMS. The wavenumbers of the four methyl group normal vibrations to RT 601 are: ν_1 = 2905 cm^{-1}, ν_2 = 2963 cm^{-1}, ν_3 = 1263 cm^{-1}, and ν_4 = 1412 cm^{-1}. To SLM 77522, they are ν_1 = 2905 cm^{-1}, ν_2 = 2963 cm^{-1}, ν_3 = 1261 cm^{-1}, and ν_4 = 1412 cm^{-1} respectively. The calculated results with experimentally observed band positions for core and cladding are summarized in Tab. 3.2 for the overtone vibrational band assignments.

Table 3.2A *Spectral positions of CH_3-group vibrations in NIR and VIS region. S, m, and w indicate strong, medium or weak absorption for a given band*

Assignment	***Cladding***		***Core***		***Intensity***
	λ /nm	***λ_{exp} /nm***	***λ /nm***	***λ_{exp} /nm***	
$\nu_1+\nu_3$	2402	2402	2402	2402	s
$\nu_2+\nu_3$	2372	2372	2372	2372	s
$\nu_2+\nu_4$	2295	2295	2295	2295	s
$\nu_1+2\nu_3$	1853	1849	1852	1851	m
$\nu_2+2\nu_3$	1837	1839	1836	1835	m
$\nu_2+\nu_3+\nu_4$	1783	1783	1784	1784	m

$2\nu_1$	1746	1746	1746	1746	s
$\nu_1+\nu_2$	1746	1746	1744	1744	s
$2\nu_2$	1703	1703	1703	1703	s
$\nu_1+3\nu_3$	1515	1539	1512	1539	m
$\nu_2+3\nu_3$	1506	1526	1503	1526	m
$2\nu_1+\nu_4$	1401	1401	1403	1403	m
$2\nu_2+\nu_4$	1376	1371	1377	1369	m
$3\nu_1$	1183	1186	1183	1186	m
$3\nu_2$	1146	1152	1146	1148	m
$2\nu_1+3\nu_3$	1063	1094	1061	1091	w
$3\nu_1+\nu_3$	1029	1020	1029	1019	w
$4\nu_1$	901	907	901	908	w
$2\nu_1+2\nu_2$	906	897	906	904	w
$4\nu_2$	868	880	868	877	w
$5\nu_1$	731	741	731	742	w
$3\nu_1+2\nu_2$	742	730	742	728	w
$5\nu_2$	701	715	701	709	w
$6\nu_1$	620	633	620	632	w

Furthermore, the higher overtone and combination bands of other vibrations with involvement of CH containing groups' vibrations in RT 601 and SLM 77522 i.e. methylene group, vinyl group and phenyl group etc. are also assigned from the NIR spectrum shown in Fig. 3.6. Results are summarized in Tabs. 3.2B, C and D respectively. From the assignment table, it can be pointed out that the absorption loss near 850 nm- the most used wavelength for datacom transmission in multimode waveguide system- is mainly due to the 3rd overtone of C-H asymmetric stretching in vinyl group and 3rd overtone of CH in phenyl group.

Table 3.2B *Spectral positions of CH_2-group vibrations in NIR and VIS region*

Assignment	λ_{exp} /nm	$\tilde{\nu}_{exp}$ /cm^{-1}	Intensity
$\nu_1+\nu_3$	2330	4290	s
$2\nu_1$	1789	5408	m
$2\nu_2$	1735	5408	s
$2\nu_1+\nu_3$	1426	7013	m
$3\nu_1$	1214	8237	w
$3\nu_2$	1181	8489	m
$4\nu_1$	918	10893	w
$4\nu_2$	895	11173	w
$5\nu_1$	754	13263	W
$5\nu_2$	719	13908	W
$6\nu_1$	637	15699	W

Table 3.2C *Spectral positions of vinyl group vibrations in NIR and VIS region*

Assignment	λ_{exp} /nm	$\tilde{\nu}_{exp}$ /cm^{-1}	Intensity
ν_1 (-CH_2) +ν_3(=CH_2)	2350	4255	S
ν_1 (-CH_2) +ν_1(C=C)	2195	4560	M
ν_1 (C=C)+ν_1(=CH_2)	2145	4660	M
$2\nu_1$	1673	5977	S
$2\nu_2$	1650	6061	M
$3\nu_1$	1144	8741	W
$3\nu_2$	1133	8826	M
$4\nu_1$	871	11481	W
$4\nu_2$	847	11737	W
$5\nu_1$	728	13736	W
$5\nu_2$	708	14124	W

$6\nu_1$	624	15949	W

Table 3.2D *Spectral positions of CH (phenyl group) vibrations in NIR and VIS region*

Assignment	λ_{exp} */nm*	$\tilde{\nu}_{exp}$ */cm^{-1}*	*Intensity*
$2\nu_1$	1690	5917	s
$2\nu_1$*(CH stret.)+*ν_2*(CH bend)*	1461	6845	m
$2\nu_1$*(CH stret.)+*$2\nu_1$*(C-C stret.)*	1425	7018	m
$3\nu_1$	1151	8688	m
$4\nu_1$	853	11723	w
$5\nu_1$	711	14065	w
$6\nu_1$	628	15924	w

3.4.3 Estimation of Absorption Loss

Estimations of the absorption loss in amorphous acrylic based polymers have been carried out by several authors, providing detailed procedures for such calculations. However, their empirical equations were deduced for acrylic polymers, using additionally the assumption of same band shapes of the absorption bands. Thus, it was our intention to derive an optical loss equation that is applicable for siloxane-based materials, considering the integrated band intensities.

In order to evaluate the maximum optical losses D_{max} in terms of dB/ cm, the integral band strengths have to be correlated with the corresponding absorption loss. An equation for the integral band strength (in cm/mol) for C-X stretching vibrations (X= H, D, Cl and F, and aromatic C-H) in dependence of the integral band absorbance, as well as for the ratio of the integral band strengths of overtones to the related fundamental vibration were derived by Groh. Under the assumption that the same band shape, but different half-widths for the calculated overtone vibrations existed, his equations were used by us, using the following expression: [17]

$$D_{\max} = \alpha \frac{\rho}{M_G} \frac{n_c}{\Delta\bar{\nu}} \frac{E_v^{CX}}{E_1^{CH}} \text{ in dB/ cm,} \qquad (3.11)$$

where a is a constant, r (g/ cm^{-3}) is the density of the polymer, M_G (g/ mol) is the

molecular mass of the polymer repeat unit, n_c is the number of C-X bonds in this repeat unit, $\Delta\tilde{n}$ is the band half-width in cm^{-1}, and E_v^{CX}/E_1^{CH} is the ratio of the band strength of the C-X vibration overtone and that of the fundamental C-H vibration band.

According to the near-infrared loss spectrum of core PDMS, we selected two similar shape overtone bands for comparison and calculation, i.e., the $4\nu_1$ and $5\nu_1$ overtones of the CH_3-group vibrations (Figs. 3.7A and B). The maximum optical loss of D_{max} ($4\nu_1$) and D_{max} ($5\nu_1$) can be measured from these spectra, for which values of about 0.601 and 0.049 dB/ cm were found. The estimated band half-widths are 86.07 and 208.6 cm^{-1} respectively from its curve fitting spectra ranging from 600 nm to 1250 nm shown in Fig. 3.8 A and B. The detailed assignment and band half-widths etc. in the wavelengths are also summarized in Table 3.3A and B respectively.

The density of cured core PDMS SLM 77522 is ρ= 0.98 g/ cm^3, the number of C-H bonds is six and the molecular mass of the PDMS repeat unit is 74 g/ mol. In addition, referring to the corresponding theoretically calculated values of E_v^{CH}/E_1^{CH} for the $4\nu_1$ and $5\nu_1$ overtones of the CH_3-group vibration, i.e. $7.2\cdot 10^{-4}$ and $9.1\cdot 10^{-5}$, respectively, and then substituting these parameters together with the experimentally derived optical loss values within the last equation, the constant a is calculated to be $0.906\cdot 10^6$ and $1.41\cdot 10^6$, providing an average value of $1.15\cdot 10^6$. The latter value is used for defining the relationship between the maximum optical loss and the band strength ratio, which can be summarized as:

$$D_{\max} = 1.15\ 10^6\ \frac{\rho}{M_G}\ \frac{n_c}{\Delta\tilde{n}}\ \frac{E_v^{CH}}{E_1^{CH}}\quad dB/cm \tag{3.12}$$

To check the equation's applicability, optical loss due to the $3\nu_1$ overtone of the CH_3 group vibration is measured and identified to have band half-width of 87.19 cm^{-1}. Based on the equation above and the theoretical value of E_v^{CH}/E_1^{CH} the calculated value is 7.10 dB/ cm compared with the measurement result of 6.98 dB/ cm. This result means that the agreement between experiment and theoretical calculation is astonishingly satisfactory.

Additionally, with respect to the PDMS core material, the optical loss at 850 nm –the most used operation wavelength for datacom- is measured to be 0.019 dB/ cm from its loss spectra shown in Fig. 3.6, and the loss of molecular vibration at 853 nm is measured to be 0.0144dB/ cm from fitting curve Fig. 3.8B, whilst in the wavelength the electronic absorption can be neglected for it is far away with the

absorption band in UV region, so we can conclude the rayleigh scattering in the wavelength is 0.0046 dB/ cm.

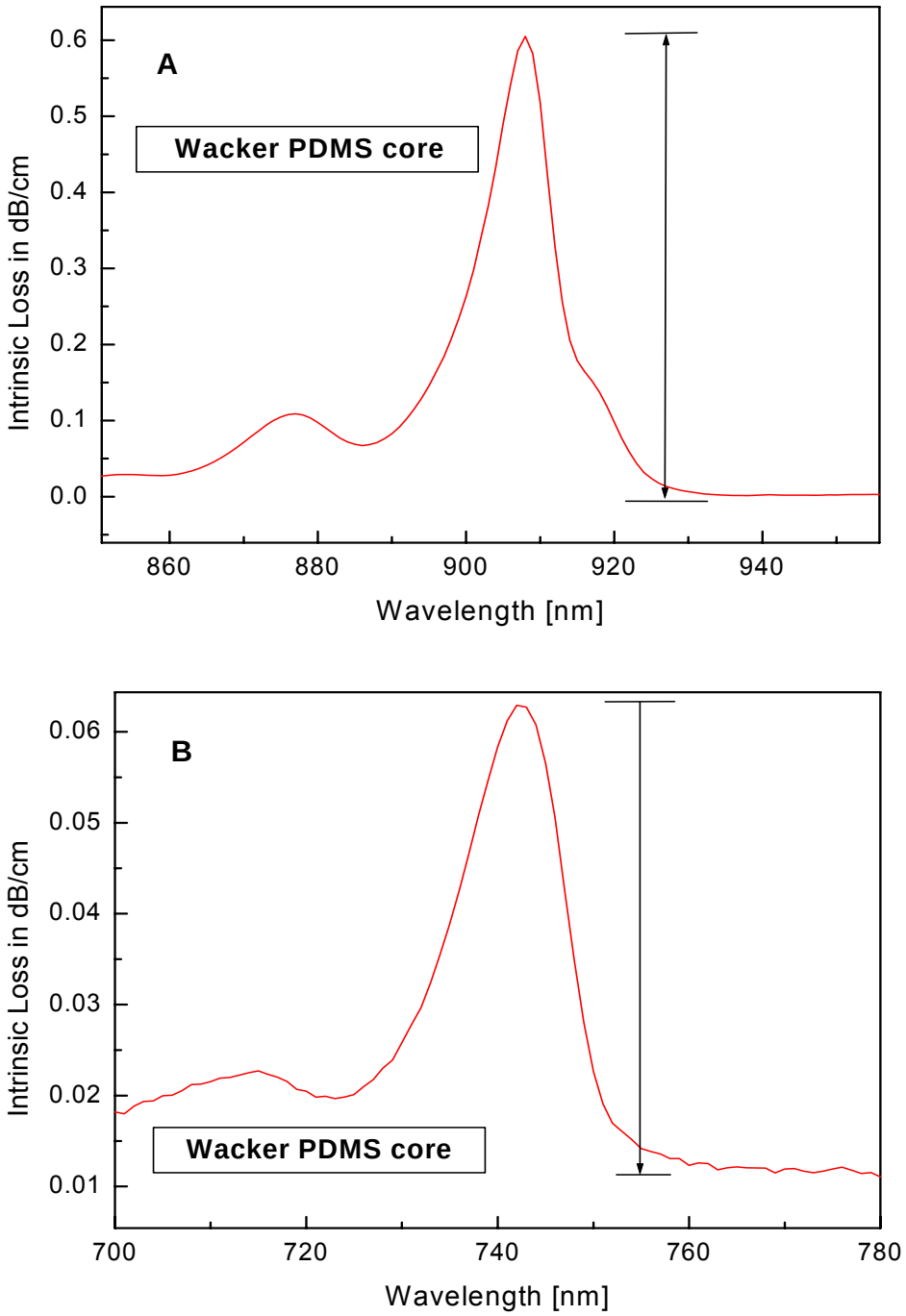

Fig. 3.7 *A and B $4\Pi_1$ and $5\Pi_1$ overtones of the CH_3-group vibrations in loss spectra*

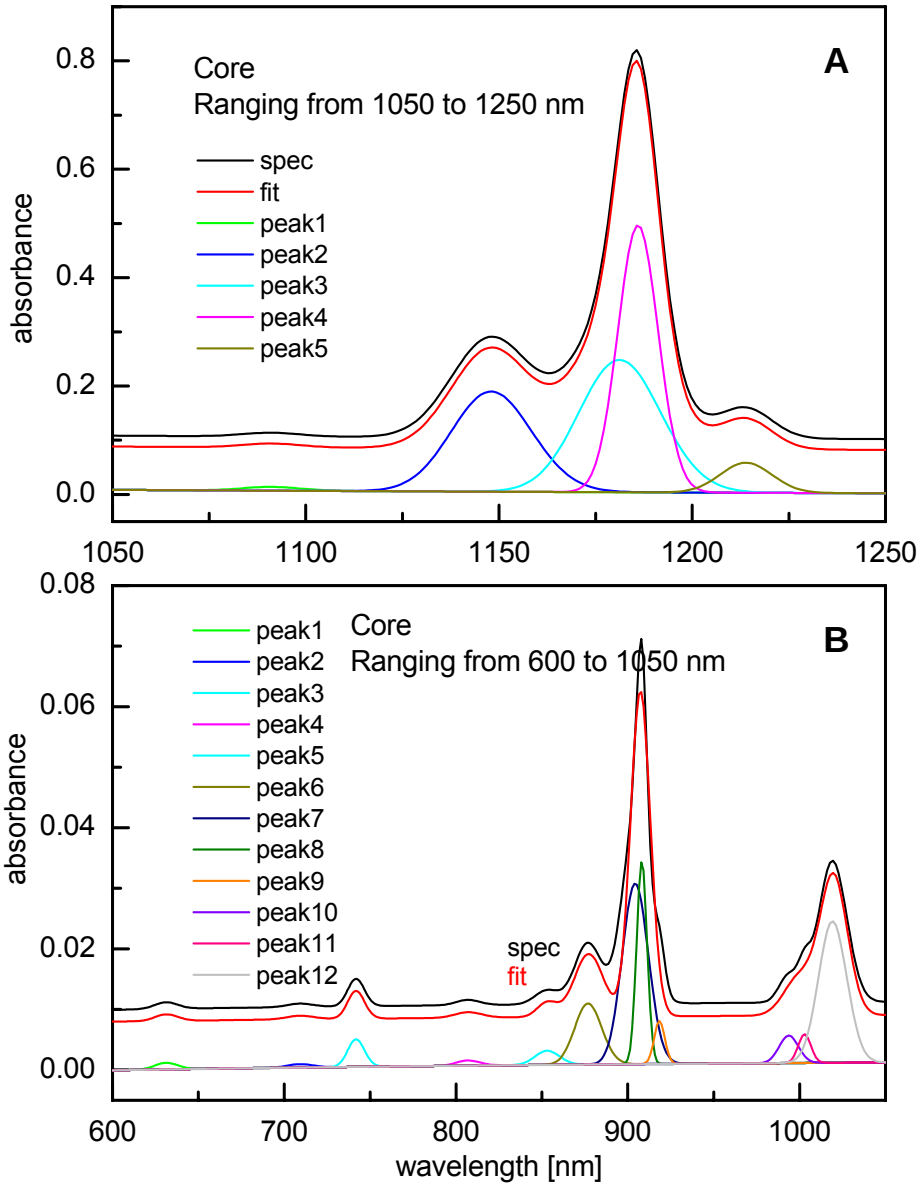
A
Core
Ranging from 1050 to 1250 nm
spec
fit
peak1
peak2
peak3
peak4
peak5
absorbance
0.0
0.2
0.4
0.6
0.8
1050
1100
1150
1200
1250
B
Core
Ranging from 600 to 1050 nm
peak1
peak2
peak3
peak4
peak5
peak6
peak7
peak8
peak9
peak10
peak11
peak12
spec
fit
absorbance
0.00
0.02
0.04
0.06
0.08
600
700
800
900
1000
wavelength [nm]

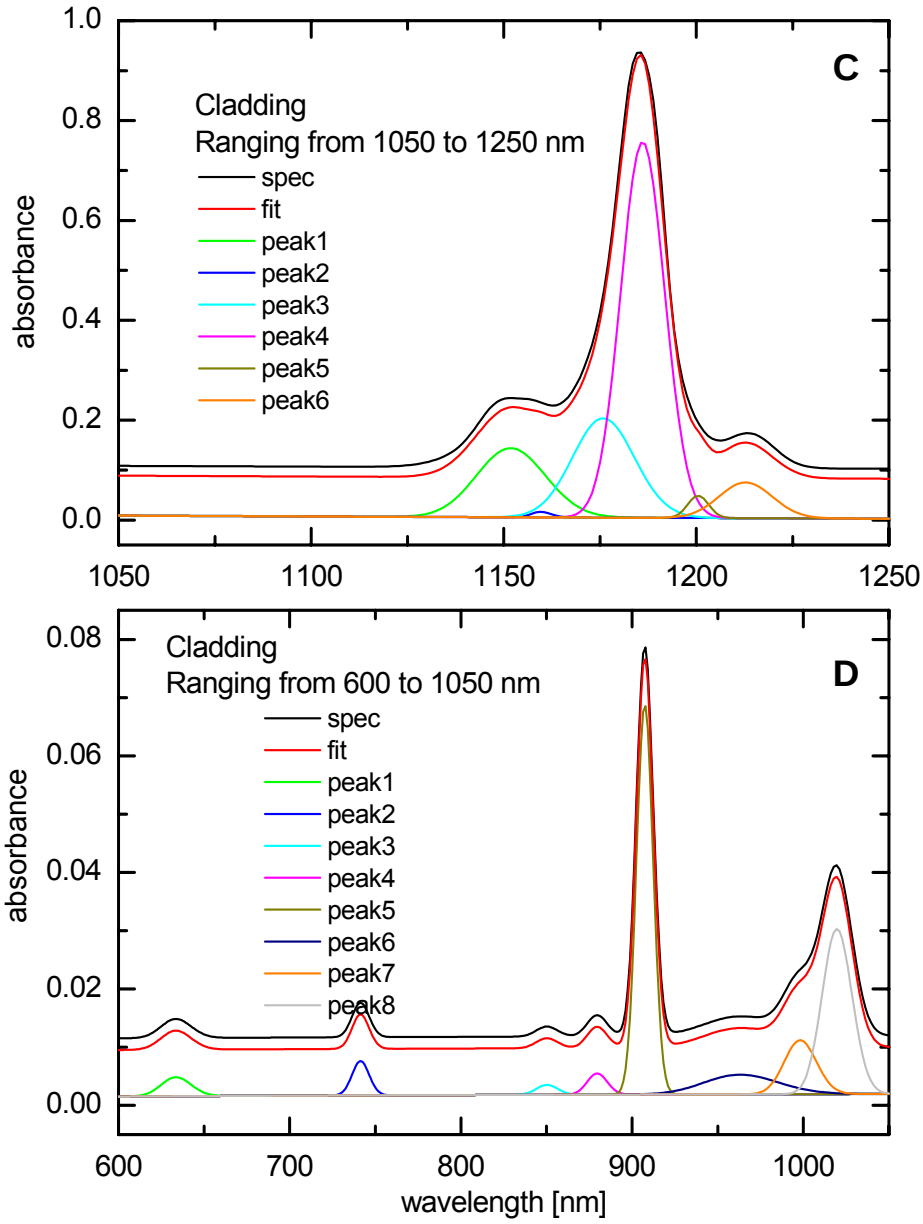

Fig. 3.8 *Curve fitting of PDMS core (A and B) and cladding (C and D) absorbance spectra ranging from 600 to 1250 nm*

According to the near-infrared loss spectrum of cladding PDMS, we also selected two similar shape overtone bands for comparison and calculation, i.e., the $4n_1$ and $5n_1$ overtones of the CH_3-group vibrations for study. The maximum optical loss of D_{max} ($4n_1$) and D_{max} ($5n_1$) can be measured from these spectra, for which values of about 0.599 dB/ cm and 0.0504 dB/ cm were found. The band half-widths are also

found to be 138.83 and 214.03 cm^{-1} respectively from the curve fitting spectra ranging from 600 nm to 1250 nm shown in Fig. 3.8 C and D. The detailed assignment and band half-widths etc. in the wavelengths are summarized in Table 3.3C and D respectively.

The density of cured cladding PDMS RT 601 is ρ= 1.02 g/ cm^3, the number of C-H bonds is six and the molecular mass of the PDMS repeat unit is 74 g/ mol. In addition, referring to the corresponding theoretically calculated values of E_v^{CH}/ E_1^{CH} for the $4\nu_1$ and $5\nu_1$ overtones of the CH_3-group vibration, i.e. $7.2\cdot 10^{-4}$ and $9.1\cdot 10^{-5}$, respectively, and then substituting these parameters together with the experimentally derived optical loss values within the last equation 3.11, the constant a is calculated to be $1.40\cdot 10^6$ and $1.43\cdot 10^6$, providing an average value of $1.415\cdot 10^6$. The latter value is used for defining the relationship between the maximum optical loss and the band strength ratio, which can be summarized as:

$$D_{\max} = 1.415\ 10^6\ \frac{\rho}{M_G}\ \frac{n_c}{\Delta n}\ \frac{E_v^{CH}}{E_1^{CH}}\quad dB/cm \qquad (3.13)$$

To check the equation's applicability, also the measured optical loss due to the $3\nu_1$ overtone of the CH_3 group vibration, with an fitted band half-width of 116.13 cm^{-1}, is also compared with the calculated results based on the equation above and the theoretical value of E_v^{CH}/ E_1^{CH}. The measured loss is 6.34 dB/ cm, taking into account band overlap from the neighboured band, while the calculated value is 6.8 dB/ cm. Like core material, this result means that the agreement between experiment and theoretical calculation is also very good.

Table 3.3A *Peak report of core material (From 1050 nm to 1250 nm)*

Gaussian	*Assignment*	*Area FIT*	*Peak center (nm)*	*Height*	*Half Width (cm^{-1})*
Peak 1	$2\nu_1+3\nu_3$ (CH_3)	1.11	1091	0.0070	149.11
Peak 2	$3\nu_2$(CH_3)	36.38	1148	0.19	184.90
Peak 3	$3\nu_2$(CH_2)	46.27	1181	0.24	177.91
Peak 4	$3\nu_1$(CH_3)	45.77	1186	0.49	87.19
Peak 5	$3\nu_1$(CH_2)	6.26	1214	0.055	106.33

Table 3.3B *Peak report of core material (From 600 nm to 1050 nm)*

Gaussian	Assignment	Area FIT	Peak centre (nm)	Height	Half Width (cm^{-1})
Peak 1	$6n_1(CH_3)$	0.47	631	0.010	399.77
Peak 2	$5n_2(CH_3)$	0.21	709	0.0056	349.77
Peak 3	$5n_1(CH_3)$	1.00	742	0.045	208.62
Peak 4	$5n_1(CH_2)$	0.23	807	0.00087	245.43
Peak 5	$4n_1$(Ar) $4n_2$(Vinyl)	0.57	853	0.0023	229.51
Peak 6	$4n_2(CH_3)$	2.57	877	0.01	239.42
Peak 7	$2n_1+2n_2\,(CH_3)$	6.94	904	0.030	218.26
Peak 8	$4n_1(CH_3)$	3.07	908	0.034	86.07
Peak 9	$4n_1(CH_2)$	0.65	918	0.0071	86.24
Peak 10	N.A	0.64	994	0.0046	132.03
Peak 11	N.A	0.44	1003	0.0048	85.68
Peak 12	$3n_1+n_3\,(CH_3)$	4.63	1019	0.023	186.01

Table 3.3C *Peak report of cladding material (From 1050 nm to 1250 nm)*

Gaussian	Assignment	Area FIT	Peak center (nm)	Height	Half Width (cm^{-1})
Peak 1	$3n_2(CH_3)$	23.33	1152	0.14	158.36
Peak 2	$3n_1$(Ar)	0.54	1160	0.011	45.01
Peak 3	$3n_2(CH_2)$	29.04	1176	0.20	137.04
Peak 4	$3n_1(CH_3)$	76.32	1186	0.75	116.13
Peak 5	$2n_1+n_2$ (CH_3)	2.10	1200	0.45	44.08
Peak 6	$3n_1(CH_2)$	8.39	1213	0.072	110.25

Table 3.3D *Peak report of cladding material (From 600 nm to 1050 nm)*

Gaussian	Assignment	Area FIT	Peak center (nm)	Height	Half Width (cm^{-1})

Peak 1	$6\nu_1(CH_3)$	1.79	633	0.0033	514.38
Peak 2	$5\nu_1(CH_3)$	1.34	741	0.0059	214.03
Peak 3	$4\nu_1$(Ar) $4\nu_2$(Vinyl)	0.37	847	0.0017	202.05
Peak 4	$4\nu_2(CH_3)$	0.69	880	0.0036	178.17
Peak 5	$4\nu_1(CH_3)$	9.88	907	0.067	138.83
Peak 6	N.A	1.97	963	0.0034	545.73
Peak 7	N.A	2.18	998	0.0093	220.74
Peak 8	$3\nu_1+\nu_3(CH_3)$	5.94	1020	0.028	196.61

Based on the measured optical loss and its theoretical calculation, PDMS will be a very good choice - owing to its low cost, easy mass production and high thermal stability - for short haul data communication application (from several centimetres to one meter) like Electrical-Optical-Circuit-Boards (EOCB) or some short distance interconnections. However, once also relatively longer distances need to be served, PDMS has to be modified for decreasing the relatively high optical loss from overtone and combination band absorption in the visible/near-infrared (VIS-NIR) region. Presently, deuteration and halogenation are the main two options to decrease the optical loss, since the CD and CX (halogen elements, e.g. F, Cl etc.) fundamental absorption bands (in particular, the stretching vibrations) in the mid-infrared region are shifted to longer wavelengths (ν(CD): 2230 cm^{-1}, ν(CF): 1250 cm^{-1} and ν(CCl): 770 cm^{-1}). Notably, also smaller anharmonicity constants exist compared with CH bond vibrations, so that finally a much lower optical loss will result for the VIS-NIR region.

After obtaining the correlation equation above and in combination with the detailed calculation results, as previously published for the ratios of E_v^{CX}/ E_1^{CH}, we can roughly estimate also the optical loss in deuterated or halogenated core PDMS within the VIS-NIR region. For example, $4\nu_1$ of the CD-stretching vibration is located at 1160 nm and the E_4^{CD}/ E_1^{CH} ratio is $1.3\cdot 10^{-4}$, and assuming its band half-width of 150 cm^{-1} being similar to that of $4\nu_1$ of the C-H bond vibration, we can find the corresponding CD stretch overtone loss value to be only 0.109 dB/ cm. This must be compared with the $3\nu_1$ of the CH-stretching vibration located at 1183 nm, as discussed above for the normal isotopic material with its optical loss found about 60 - 70 times larger than for the $4\nu_1$ of CD stretch overtone loss. Whilst from

a theoretical view deuteration and halogenation in siloxane-based materials are proving their applicability to render even more transparent materials, practical aspects about the use of such materials must still be investigated.

In addition, in terms of core PDMS and with respect to the siloxane polymer design, assuming a ratio of ρ / M_G = 0.01 mol/ cm^{-3} based on possible deuteration or halogenation and n_c = 6, an absorption loss of 0.001 dB/cm could be achieved when referring to a quotient of $E_v^{CX} / (E_1^{CH} \cdot \Delta\bar{n})$ of $1.09 \cdot 10^{-8}$. Furthermore, specifically to 850 nm, the optical loss at 850 nm of polysiloxanes will be mainly from rayleigh scattering e.g. 0.0046 dB/ cm to PDMS SLM core material once the absorption peaks near 850 nm are shifted due to deuteration or halogenation, therefore the inhomogeneities in polysiloxanes should be also controlled to obtain higher optical transparency, e.g Pt catalyst concentration and curing conditions etc. After knowing the optical loss limit, it is very important and helpful for the optical material design for decreasing the loss by appropriate hydrogen substitution, but even amplification (which can be reached with doping the PDMS material with some rare-earth metal materials showing luminescence at the requested signal wavelength) may be necessary.

3.5 Processing of PDMS Waveguides

The technique and relevant issues for processing polymer optical waveguides are quite similar to those for polymers in microelectronic packaging. Spin coating, doctor blading, extrusion and lamination etc. are all the normal techniques for casting polymer films. Then it differs with their application in microelectronic packaging, in waveguide fabrication it concerns more on film uniformity and controllable desirable thickness, free of bubbles and striations, and adhere to substrates or not etc.

Furthermore, in general, waveguide fabrication by means of replication techniques comprises the following steps:
-Fabrication of a mould with the desired waveguide pattern in form of ridges;

-Replication of the waveguide pattern into a polymer substrate which contains the waveguide structure in form of grooves;

-Filling of the grooves by a liquid core polymer which has a higher refractive index than the substrate and subsequent curing of the core polymer by UV-light or heat.

3.5.1 Fabrication of PDMS Optical Waveguides

It is well known that several properties of PDMS material are instrumental in the formation of high-quality patterns and structures. First it shows extremely high temperature stability with respect to material degradation as well as to optically transparent down to about 300 nm. Second, PDMS is one typical elastomer and can conform to the surface of the mould over a relatively large are and is excellent materials for replication processes since they can be released easily from moulds, even from complex and fragile structures, and are able to replicate structures down to the nm-range due to its elastic characteristic. Third PDMS provides a low surface energy surface when it is cured (ca. 21.6×10^{-3} J/ m^2) and chemically inert, in addition its surface properties can be readily modified by thermal treatment, UV/ O_3, gas plasma and chemical treatments to give requested interfacial properties based on different requirements. [65]

For fabrication of waveguides by using this optical material, casting is adopted as the suitable technology with regard to the PDMS properties. The first basic prerequisite for the replication process is a robust mould or stamp with low sidewall surface roughness (< 30 nm) to guarantee a low scattering loss, e.g. 6” Nickel casting mould in Fig. 3.9.

The fabrication starts by filling the waveguide grooves with the liquid core polymer which is done using a blading process (Fig. 3.10a). The choice of PMMA or POM as blading material was guided by the demands of the blade softness, flexibility, but long lasting endurance. This process step is finished by thermal curing of the core polymer. As the second step, liquid cladding material is poured onto the whole mould area (Fig. 3.10b). After curing, first cladding and core are together separated from the mould (Fig. 3.10c). This half-open structure is then filled with cladding material (second cladding). A final curing step d terminates the production process of the wave guiding laminate and after this and the optical layer can be packaged.

In the single mode fabrication, due to the small core size two issues are worth mentioning: one is the curing temperature which is proposed to be 70 °C, since the PDMS parts will shrink if the PDMS prepolymer is cured at higher temperature, not ensuring a satisfactory pattern transfer. The other aspect is the influence of the substrate on the crosslinking rate to the PDMS thin film (for example, below 15 μm). Simpson et al.[66] proposed that the dependence of the first-order coefficient for the PDMS hydrosilylation crosslinking reaction on the type of interface is probably the result of an interfacial segregation and complexation of the Pt catalyst.

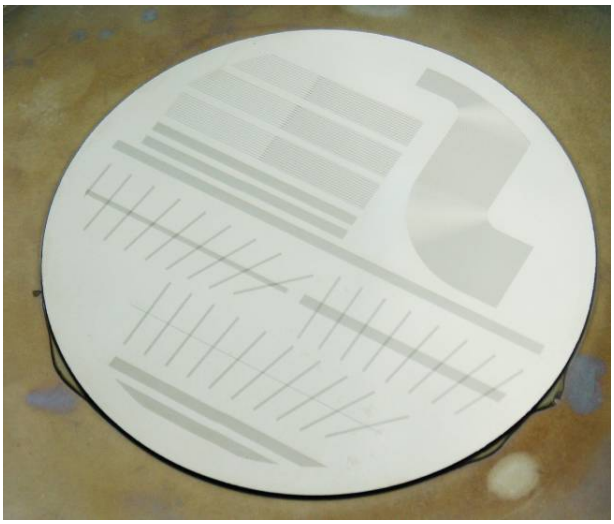

Fig. 3.9 *6" Nickel casting mould*

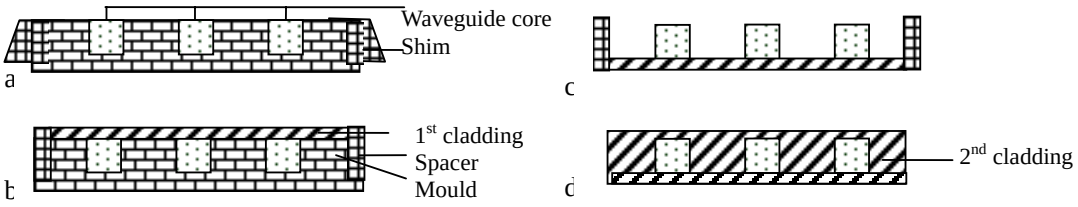

Fig. 3.10 *Schematics of the waveguide fabrication using PDMS*

Single mode

The waveguide sandwich will be cut by a razor blade at both end faces to prepare the sample for optical characterization. The cross section of a fabricated PDMS singlemode waveguides is illustrated in Fig. 3.10 which has core sizes of 6 × 6 μm^2. With these standard commercial PDMS materials (see Figure 3.11) a PDMS singlemode waveguide loss of 0.17 dB/ cm could be obtained at 1300 nm. Further reduction of transmission loss may achievable by using aforementioned introduced partially halogenated materials.

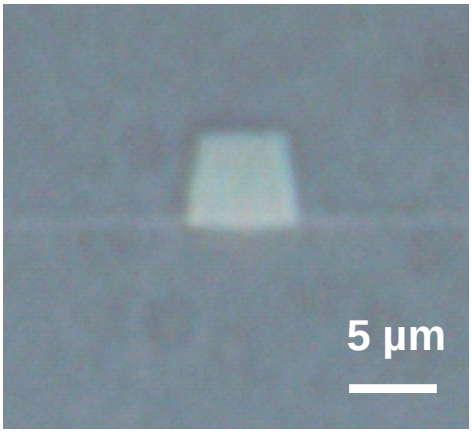

Fig. 3.11 *cross section of a fabricated PDMS singlemode waveguide*

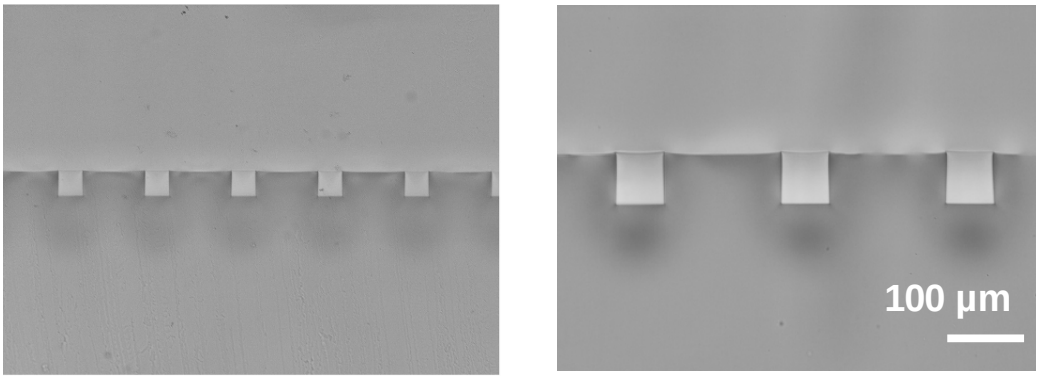

Fig. 3.12 *cross section of a fabricated PDMS multimode waveguide*

Multimode

The cross section of a fabricated PDMS multimode waveguides is illustrated in Fig. 3.12 which has core sizes of 70 × 70 µm^2.

The optical insertion loss measurement of PDMS waveguides were measured at 850 nm which is commercially used for optical datacom transmission in multimode waveguides. The detailed schematic set-up is shown in Figure 3.13.

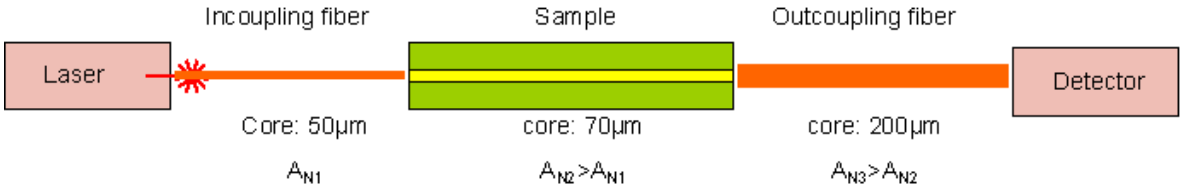

Fig. 3.13 *schematic set-up of optical loss measurement*

The instrument OMS150 of the company "Wavetek Wandel Goltermann" (Enirrgen

uA, Germany) was used for optical loss measurement, which contains of two laser sources and a detector. For our experiments a dual laser arrangement with wavelengths of 650 nm and 850 nm was applied. The spectral range was independent of the operating temperature with tolerances of ± 10 nm. The laser radiation sources were operated in the WDM mode, so that a synchronous measurement of the two wavelengths was possible. The laser light was launched into the waveguides through a butt-in-coupling 50 µm GI fibre (See Fig. 3.14) and a 200 µm SI fibre for butt-out-coupling.

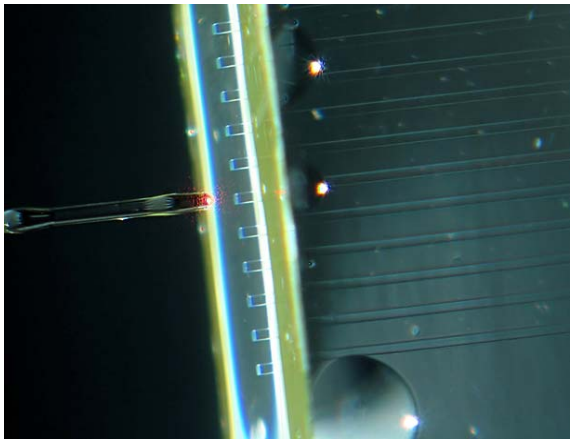

Fig. 3.14 *Measurement of PDMS waveguides insertion loss*

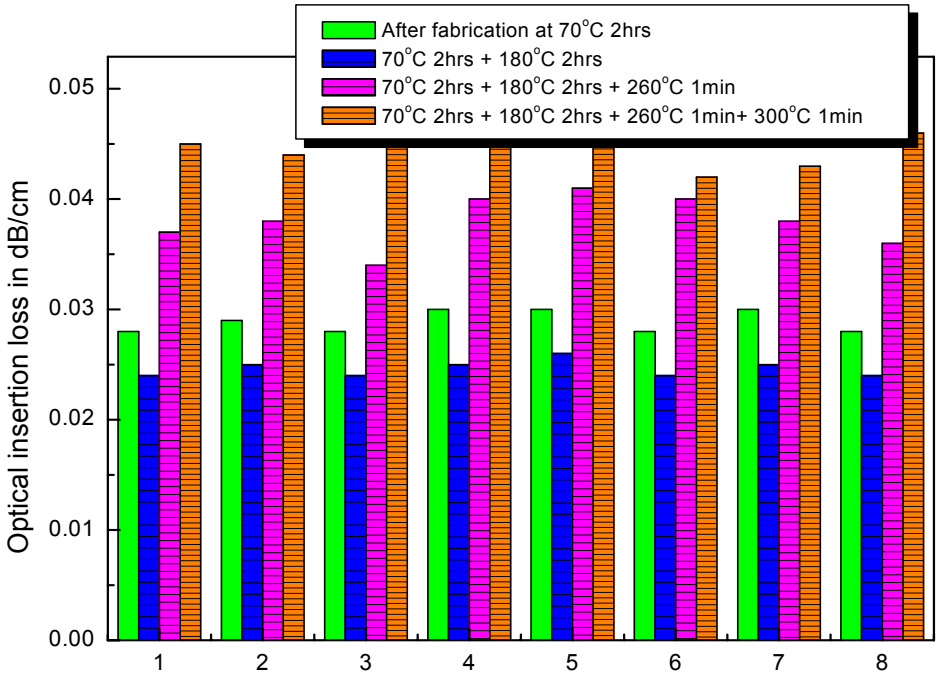

Fig. 3.15 *Optical insertion loss of PDMS multimode waveguides*

The measured optical insertion loss of PDMS waveguides after curing and different temperature treatments are shown in Fig. 3.15 and the transmission loss of multimode waveguides based on such 2 component thermal curing wacker PDMS is below 0.05 dB/ cm even after temperature treatment up to 300 °C. The optical loss after 180 °C for 2 hrs is decreased possibly due to the decrease of vinyl group concentration with the further curing of PDMS. Summarily, it proves such PDMS material appropriate for short distance optical data transmission in even high temperature environments replacing other thermal modified high cost optical polymers such as acrylate and epoxy-based materials.

3.5.2 Scattering Loss from Mould Roughness

Like aforementioned, core–clad interface roughness is another source of extrinsic loss. Actually, except scattering loss, roughness and inhomogeneity also can generate unwanted mode coupling and modulation of mode coupling in devices and beating/ coupling length. Thus extrinsic loss in waveguide system typically result from core–clad interface roughness needs to be identified. Referring to the casting method for PDMS waveguide fabrication, actually the interface roughness is the copy of grooves and defects from the sidewalls of casting moulds. Additional attenuation (scattering loss) which is from continuous coupling from bound modes to the radiation field may be caused due to these surface defects and roughness. A white-light-interferometer named Veeco NT 1000 is used to quantify the roughness of casting moulds (Fig. 3.16) and SEM is adopted for direct topography observation (Fig. 3.17).

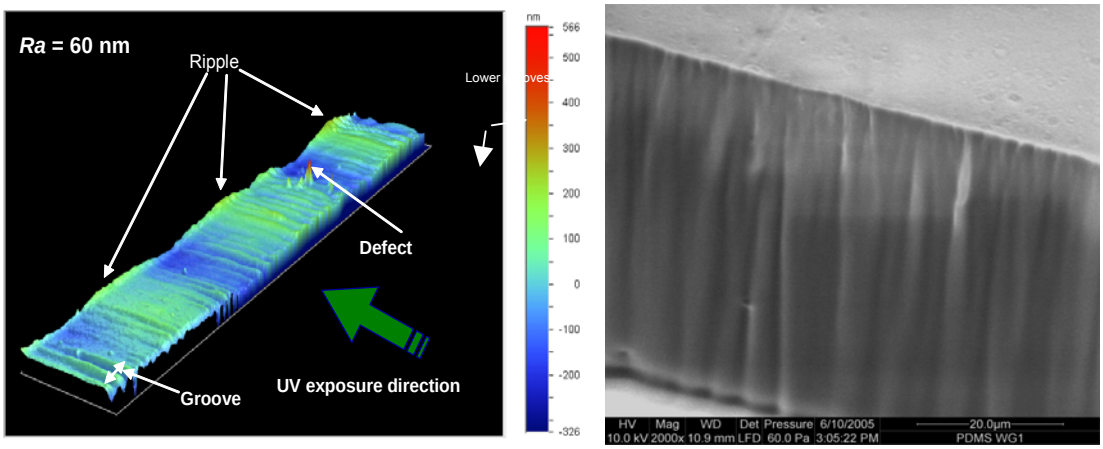

Fig. 3.16 Roughness of casting mould sidewall **Fig. 3. 17** Topography of casting mould sidewall

The optical intrinsic absorption of core and cladding PDMS are measured with NIR

spectrometer and the spectra are illustrated in Fig. 3.6 already. From their NIR spectra, the largest optical losses in the region from 842 to 855 nm where measurement laser will work are measured and calculated based on Lambert' law. Optical intrinsic loss of PDMS core is 0.0192 dB/ cm and cladding loss is 0.0176 dB/ cm respectively, which core material has relatively higher loss than cladding possibly due to its higher concentration of phenyl group whose 3rd overtone of Ar-CH is just in that region.

Additionally, in such cross-section PDMS waveguide system (RI of cladding and core: 1.4041 and 1.4275 at 589 nm and 20 ^{o}C), to simplify the calculation of waveguide loss attributed to PDMS, considering 10 % light will transmit in cladding layer it is assumed that 90 % contribution of waveguide loss is from core material and the other 10 % is from cladding Hence, the waveguide loss is 0.01904 dB/ cm.

Differently qualified SU-8 casting moulds are fabricated from different masks which directly determinate the sidewall surface qualities of moulds. Their roughness is quantified with Veeco NT 1000, where 10 spots are measured per waveguide; in addition PDMS optical waveguides of 8 cm length are fabricated based on these different quality moulds. The optical insertion loss of these obtained PDMS waveguides with different core-clad interface roughness are measured at 850 nm wavelength. Compared with sidewall roughness, the top and bottom interfaces between core and cladding can be neglected. Hereby we consider the interface roughness is main from the two sidewalls between them, in addition it is also assumed the edge qualities of lines in every mask are identical. Theoretically, the optical propagation loss due to scattering will be increased evidently when average roughness of waveguide sidewalls is more than λ(wavelength)/ 20, and hence to 850 nm wavelength, the critical transition Ra is 42.5 nm, and from the measured diagram shown in Fig. 3.18, the experimental critical transition Ra is about 50 nm.

Also, from the diagram it can help us determine the quality of mask based on different optical quality requirements to PDMS waveguides because the mould roughness is directly related with the mask. For example, supposed optical waveguide loss to be less than 0.05 dB/ cm, the average roughness of casting mould should be controlled below 40 nm and thus relevant quality mask should be selected.

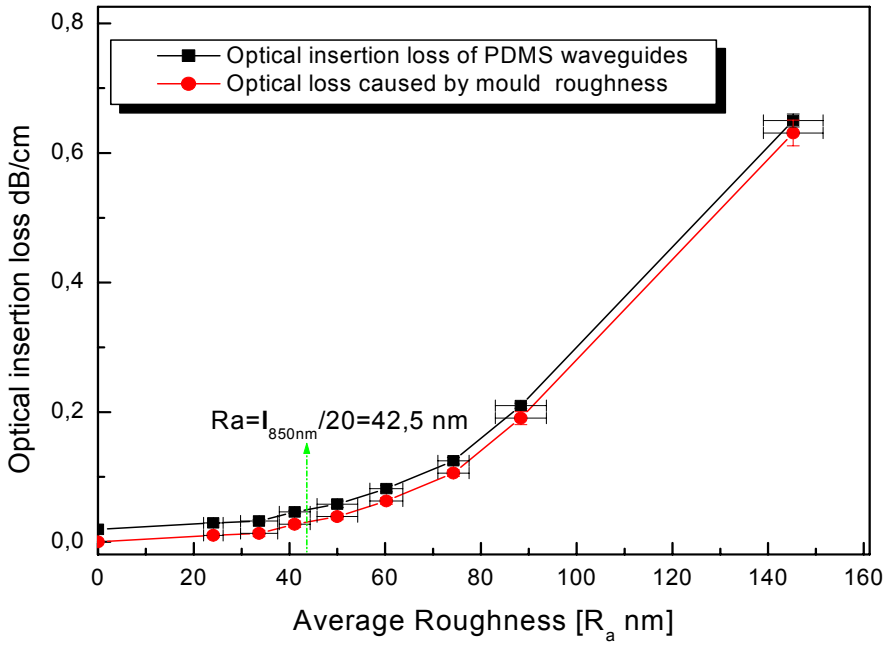

Fig. 3.18 *Relationship between sidewall roughness and optical waveguide loss at 850 nm*

3.5.3 Optical Loss due to Interlayer

Based on PDMS casting technique, the interlayer will form if over filling PDMS core and incomplete blading etc. (See Fig.3.19). Mainly the interlayer may be divided into two kinds, one is structure 3.20B in Fig.3.20, where two waveguides or more are connected by the interlay which causes the optical crosstalk and brings extra optical loss consequently, and the other is pure interlayer i.e. no connection with other waveguides: structure 3.20C, though no caused crosstalk due to it, it will lead to some extra mode dispersion and some light into cladding layer, and ultimately bring optical loss.

In the part, through modifying flatness of casting mould and blading pressure and angle etc., different thick interlayers are formed and respectively the thicknesses of different interlayers are measured by ellipsometer. Additionally, the fabricated waveguides are characterized with optical laser measurement at 850 nm wavelength and the relationship between interlayer thickness and optical loss is illustrated in Fig. 3.20 also including the ray-tracing based simulation results in terms the respective interlayer thickness. Basically one good agreement is achievement. It is concluded as well that the interlayer thickness should be less 500 nm for achieving the basic low optical loss requirement.

In order to meet the basic quality requirement of optical loss, in terms of different moulds appropriate blading angle and pressure and surface treatments of casting mould are necessary to be checked and controlled experimentally, for example it is identified that blading conditions for SU8 mould are 2 bar pressure, POM material based blade and blading angle of 60° etc.

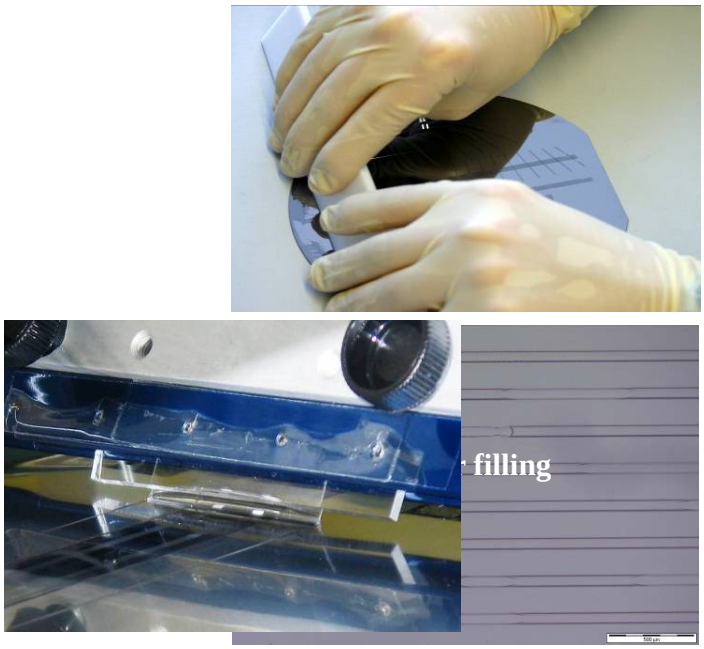

Fig. 3.19 *blading step during waveguide fabrication and overfilling due to incomplete blading*

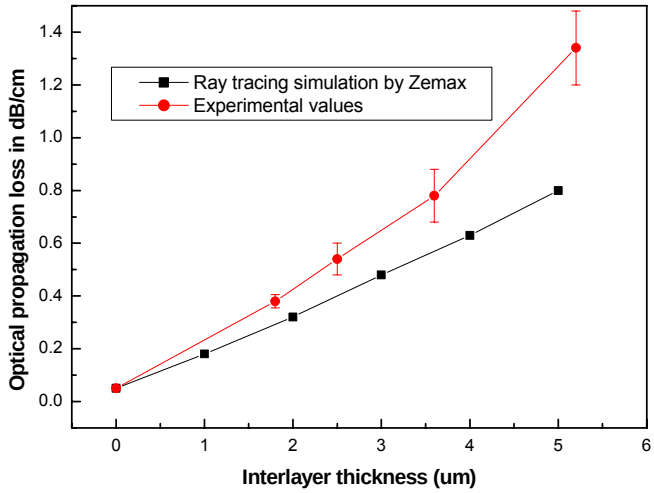

Fig. 3.20 *cross section of fabricated waveguides and interlayers*

3.5.4 Optical Loss from Packaging Substrates

Nowadays, in PCB industry, polymer based PCBs e.g. epoxy, Polyimide, PolyBenzImidazole , PolyEtherEtherKetone (PEEK), Polyester, Polycarbonate and PolyAmide-Imide are widely applied due to their good insulation properties, low cost and familiar production techniques with high stability and reliability etc., however with respect to EOCB production, their chemical compatibilities with PDMS materials of optical layer will be one important quality aspect based on EOCB production technique, e.g. outgas from heated organic PCBs.

FR4 (Glass reinforced Epoxy) series are strongly preferably recommended due to their popular use in market, low cost and familiar process and technologies etc.

As we knew, FR is the abbreviation of Flame Resistant and 4 is the class of flame retardment, and in order to improve the ability of flame retardment, some inorganic-based fillers and organic additives are added into epoxy materials in term of forms of composites and chemical synthesizing (reaction in the backbone of epoxy polymer), e.g. ATH ($Al(OH)_3$), $Mg(OH)_2$, halogen-based epoxy, phosphorous-based epoxy and nitrogenous-based epoxy etc. In order to resist flame under the condition of high temperature (e.g. lamination and soldering), they will give out various gases for preventing the flame continuous development, e.g. H_2O, noxious hydrogen halides, HPO_2, HPO and N_2 etc. as well as including some other gases from substrate materials, e.g. CO, CO_2, aromatic and alkyl CH containing gases, and even furan and dioxin etc. [67-68]

In order to identify the influences from FR4 boards on optical layer, PDMS waveguide foils without and with two different FR4 carriers (Halogen FR4 and Halogen-free FR4) kindly supported by ILFA, Hanover, Germany, are prepared based on one kind of specifically developed packaging method in our group which will be in detailed introduced in next chapter, and these fabricated waveguide laminates have dimensions of 40 × 100 mm. The thickness of PDMS layer is about 300 μm. The waveguides cross-section is 70 × 70 μm^2. The waveguide pitch is 250 μm which is from the normal pitch of commercial VCSEL-arrays. A cross-section of such PDMS waveguide foil with FR4 carrier is shown in Fig. 3.21.

After curing at 70 °C, 180 °C for 2h (simulated lamination process) and 260 °C for 1min (lead-free soldering process) optical characterization with 850 nm laser is performed again and the detailed results of the PDMS waveguides without and with different kinds of FR4 foils are illustrated in Fig. 3.22.

From the results, the influence from halogen containing FR4 is obvious and leads

to optical loss increased to be over 0.1 dB/ cm. Optical measurement (See Fig. 3.23) of PDMS core material covered with the kind of halogen FR4 board with FTNIR spectroscopy were performed before and after 180 °C for 2 hrs treatment to identify the change. From the spectrums, some increased vibrational overtone and combination bands peaks from 840 nm to 880 nm are found which also fits with aforementioned optical insertion loss measurement results.

Then, it is also observed that the optical insertion loss changes very small, when the halogen FR4 board is deposited with copper as barrier layer and the result is shown in Fig.3.24, which is for the prevention of outgas from heated halogen containing FR4 by the diffused copper.

In addition, obviously compared with PDMS waveguides without any carrier layer stress optical loss is not so important due to CTE and young's modulus mismatch between FR4 and PDMS boards. Therefore, we propose that the higher optical loss possibly is due to steam, some CH overtone and combination band vibration in double carbon bond existing gases e.g. furan and dioxin emitted from halogen FR4, for such two emitted small volume gases can easily diffuse into largely expanded PDMS matrix (CTE: 300 ppm/ K) because of their high molecular volume, which finally cause the loss due to their light absorption near 850 nm (overtone of OH, $4n_2$ (Vinyl)- 847 nm and $4n_1$ (Phenyl)- 853 nm)).

So, in the future EOCB system, the selection of organic PCB boards will also play a vital role in optical quality aspect of EOCBs, and halogen free boards are recommended. Further, one copper deposition layer may also be considered as gas-resist layer.

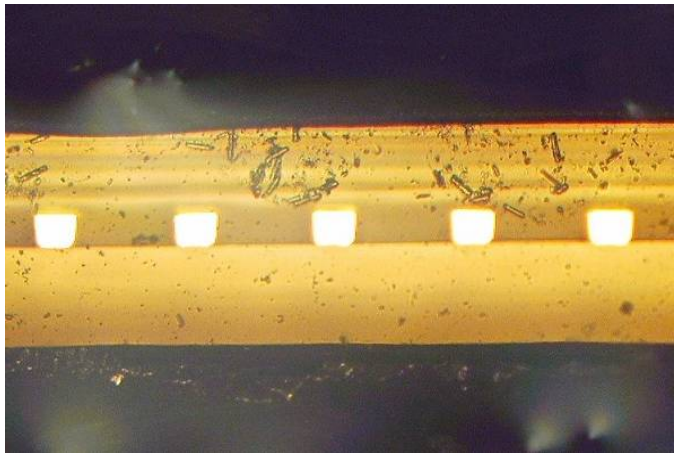

Fig. 3.21 *Cross-section of a PDMS waveguide foil with FR4 carrier*

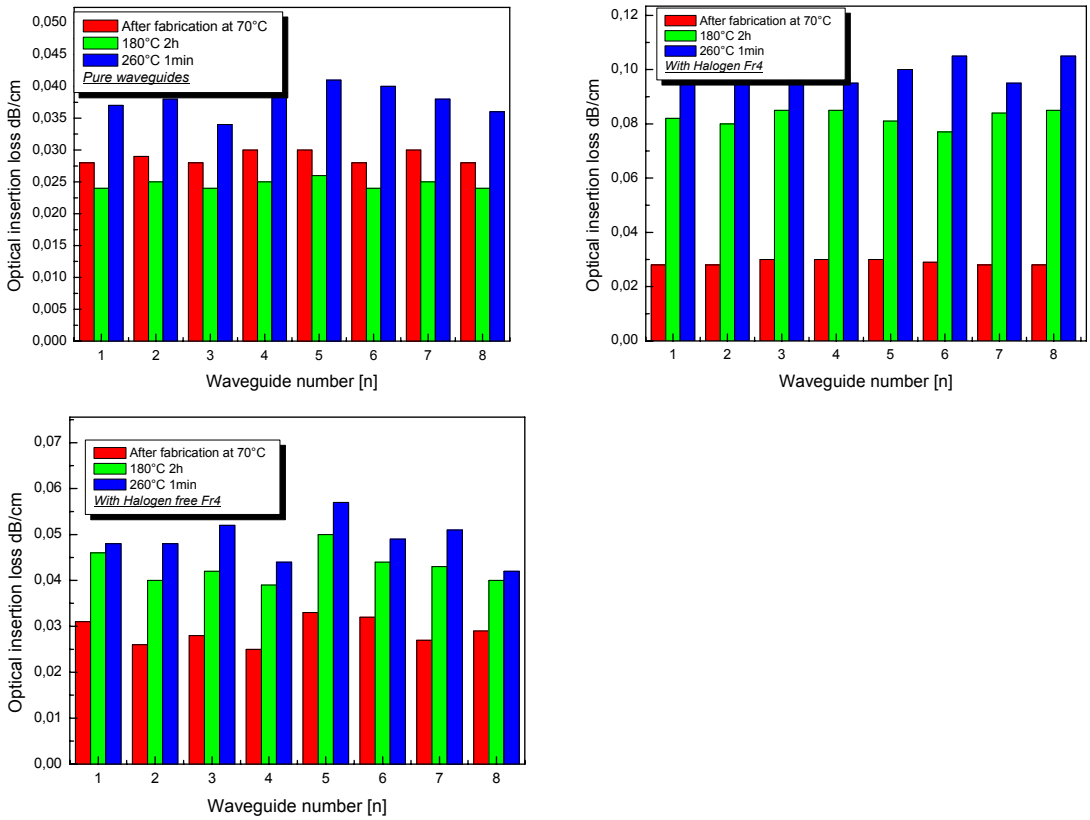

Fig. 3.22 *Optical insertion loss results of PDMS multimode waveguides without and with different carriers*

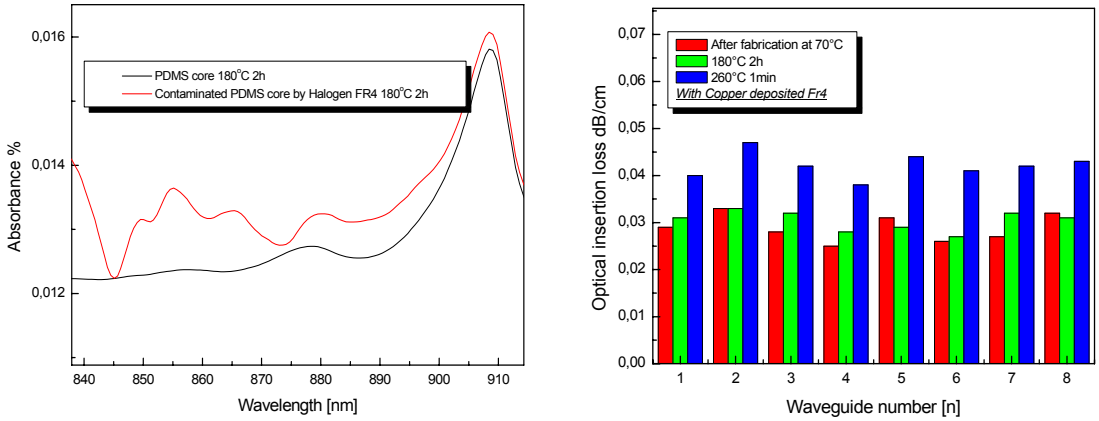

Fig.3.23 *FTNIR spectra of PDMS core material with and without cover of halogen FR4 after thermal treatment*

Fig.3.24 *Optical insertion loss of PDMS waveguides covered with copper foil FR4 boards*

3.6 Summary of results of the chapter

In the chapter, the numerical aperture of polysiloxanes based waveguides was verified to be less 0.275 and fulfilled the basic bandwidth requirement of 10 Gbps/ 1m. Additionally, considering from different operation environments and thermal conduction influences from surrounding active elements e.g. VCSEL and PD the thermal stability of numerical aperture was also verified and to be proved to be very stable.

In broad wavelengths, the optical intrinsic loss of polysiloxanes and the deterministic factors were studied both. With respect to core polysiloxane at 850 nm, which is mostly used for datacom, the optical loss is 0.019 dB/ cm and found that the loss of 0.0144 dB/ cm is from the molecular vibration and the left 0.0056 dB/ cm is from rayleigh scattering.

Furthermore, experimentally it was found that average roughness of casting mould applied in waveguide fabrication should be controlled to be less 40 nm and the interlayer thickness due to incomplete blading within waveguide fabrication should be less 500 nm in order to obtain eligible EOCBs. Also, the halogen containing packaging substrates can give out gas which will absorb optical light near 850 nm wavelength and should be neglected, and halogen-free containing boards or copper covered boards are recommended for EOCB packaging.